Diversity of biological activities of crude venom extracted from five species of South China Sea anemones

Panmin He[1†], Ming Li[1†], Jinxing Fu[1], Yanling Liao[1], Bo Yi[2]* and Bingmiao Gao[1]*

[1]Engineering Research Center of Tropical Medicine Innovation and Transformation of Ministry of Education & International Joint Research Center of Human-machine Intelligent Collaborative for Tumor Precision Diagnosis and Treatment of Hainan Province & Hainan Provincial Key Laboratory Of Research and Development on Tropical Herbs, School of Pharmacy, Hainan Medical University, Haikou, Hainan, China, [2]Department of Pharmacy, 928th Hospital of PLA Joint Logistics Support Force, Haikou, Hainan, China

Developing novel, efficient, and safe peptide drugs from sea anemones has aroused great interest in countries around the world today. Sea anemones contain complex protein and peptide toxins, which determine the diversity of their biological activities. In this study, a variety of activities were assessed for crude venom extracted from five species of South China Sea anemones, including hemolytic, enzyme inhibition, anticancer, insecticidal, analgesic and lethal activities. The most toxic sea anemone was found to be *Heteractis magnifica*, which has high lethal activity in mice with an LD_{50} of 11.0 mg/kg. The crude venom of *H. magnifica* also exhibited a range of the most potent activities, including hemolytic, trypsin inhibitory, cytotoxic activity against U251 and A549 cells, insecticidal and analgesic activities. In addition, the crude venom of *Stichodactyla haddoni* was the most effective inhibitor of pepsin, and the crude venom of *Heteractis crispa* was extremely strong toxicity to HepG2 cells. These findings are of great significance for exploring the potential and application of South China Sea anemone resources, and are expected to provide new directions and possibilities for the development of novel anticancer drugs, analgesics and biopesticides.

1 Introduction

Marine ecosystems are among the most biologically diverse and marine biomass has become an effective source for the development of innovative biotechnology, driving the discovery of new therapeutic strategies and compounds, with venom from marine animals being recognized as an emerging source of peptide-based therapeutics (Liao et al., 2019b; Melendez-Perez et al., 2023). Since the Food and Drug Administration approved the use of cytarabine for leukemia treatment, an increasing number of scientists have been motivated to invest significant efforts in the development of marine drugs (Montaser and Luesch, 2011). Currently, ziconotide extracted from *Conus magus* has been clinically approved for the treatment of chronic pain, and ShK-186, an analogue of ShK from *Bunodosoma granulifera*, now known as dalazatide, has successfully entered Phase I trials for the treatment of autoimmune diseases (Liao et al., 2019a; Coulter-Parkhill et al., 2021; Moovendhan, 2024). Despite the immense potential of marine organisms, there remains a significant gap in the number of peptide drugs extracted from non-marine species, such as eptifibatide, bivalirudin and exenatide (Koh et al., 2018; Coulter-Parkhill et al., 2023; Tonin and Klen, 2023). Therefore, more intensive and systematic research and development are urgently needed.

Sea anemones (Cnidaria, Actiniaria) are marine invertebrates and one of the oldest surviving venomous species (Madio et al., 2019; Ashwood et al., 2022). At present, approximately 1100 sea anemone species have been recorded, most of which inhabit temperate regions and some live in the tropics (Gomes et al., 2016; Fu et al., 2021). In Chinese sea areas, the distribution of sea anemone resources indicates that the South China Sea has the highest abundance, followed by the Yellow Sea, and the East China Sea has the lowest. Sea anemones survive in a variety of marine habitats, typically adhering to rocks and other objects, displaying immobility, with only a few capable of slow crawling (Kasheverov et al., 2022; Menezes and Thakur, 2022). Like all other cnidarians, sea anemones possess structures that produce microscopic venom transport, called nematocysts, venoms were produced and stored by highly specialized nematocysts (Fautin, 2009; Moran et al., 2012; Rachamim et al., 2015; Menezes and Thakur, 2022; Monastyrnaya et al., 2022). With no skeleton and lacking the most basic brain foundation or central information processing mechanism, they rely on the production of venoms to capture prey, which also perform roles for defensing, intraspecific aggressing and digesting (Frazao et al., 2012; Mitchell et al., 2021). For example, grass shrimp are predators of *Nematostella*, and studies of sea anemone venom proteomes revealed more families with neurotoxic activity than those with other modes of action, and studies have demonstrated that transgenically deficient and native *Nematostella* strain lacking a major neurotoxin have reduced defense to grass shrimp, suggesting that neurotoxins are essential in defense against invertebrate predators (Ashwood et al., 2022; Smith et al., 2023; Surm et al., 2024).

Venoms are usually a mixture of peptides, proteins and non-proteinaceous compounds. Among them, the peptide components are of great interest to scientists due to their high toxicity, diversity and structural stability. Sea anemone peptides mainly form disulfide bonds with multiple cysteine residues, forming stable structural scaffolds. So far, at least 17 different molecular scaffolds have been found in sea anemone peptides (Caswell et al., 2013; Madio et al., 2018; Pinheiro-Junior et al., 2022). In addition to exhibiting a broad range of biological activities, these venoms serve as valuable research tools for different molecular targets, currently affecting at least 20 pharmacological targets (Prentis et al., 2018; Tajti et al., 2020; Kasheverov et al., 2022; Da Silva et al., 2023). The most extensively researched sea anemone toxins are those that regulate voltage-gated sodium (Nav) and potassium (Kv) channels, acid-sensing ion channels (ASICs), transient receptor potential (TRP) ion channels, as well as toxins that inhibit polyfunctional proteases (mainly Kunitz-type) and pore-forming toxins that can interact with the plasma membrane of eukaryotic cells (Isaeva et al., 2012; Cardoso and Lewis, 2018; Leychenko et al., 2018; Prentis et al., 2018; Madio et al., 2019; Wang et al., 2021; Zhao et al., 2024). Transcriptomic and proteomic studies have shown that each sea anemone can produce approximately 1000 transcripts, with 1174 sea anemone species annotated in WORMS (https://www.marinespecies.org, accessed on 26 September 2024), it is estimated that sea anemones may be able to produce about 1,200,000 natural peptides (Fu et al., 2021; Guo et al., 2024; Li et al., 2024). However, with only about 492 sea anemone toxins annotated in UniProtKB (https://www.uniprot.org, accessed on 21 September 2024), there are still numerous undiscovered sea anemone venoms that could be developed into novel peptide medicines.

With advances in transcriptome sequencing technology, mass spectrometry instrumentation, and bioinformatics tools, a detailed overview of proteins and peptide toxins in sea anemones using transcriptomic and/or proteomic approaches has revealed the complexity of venoms (Mazzi Esquinca et al., 2023; Li et al., 2024). It had been identified from transcriptomics that *Heteractis magnifica*, *Entacmaea quadricolor*, *Stichodactyla haddoni*, and *Heteractis crispa* expressed 728, 1251, 508, and 1049 toxin-like transcripts, respectively (Madio et al., 2017; Guo et al., 2024; Hoepner et al., 2024; Li et al., 2024). However, due to the huge sequencing data, synthesizing peptides one by one has become difficult, and rapidly evaluating the pharmacological activities of synthesized peptides also faces challenges. Therefore, it is necessary to verify the activities of the five sea anemones collected from the South China Sea and select the most promising anemone resources for further study. So far, sea anemones have played a crucial role in the development of marine biotechnology. Some sea anemone venoms have been shown to possess different activities with rich medicinal value, promoting the development of marine medicines and biologics. For example, venoms of *H. magnifica*, *S. haddoni*, *Paracodylactis sinensis* and *Stichodactyla helianthus* induced spontaneous hemolysis in erythrocytes (Ravindran et al., 2010; Rivera-de-Torre et al., 2020). Moreover, enzyme inhibitors had been found in sea anemone toxins such as *Bunodosoma caissarum* and *E. quadricolor* (Mazzi Esquinca et al., 2023; Hoepner et al., 2024). Notably, sea anemone researches had also identified several venoms with anticancer activities. For example, *H. magnifica* and *E. quadricolor* venoms were cytotoxic to human lung cancer cells (A549) and toxins from *H. crispa* showed anticancer activities and

prevented HT-29 colorectal cancer cell migration (Ramezanpour et al., 2012; Kvetkina et al., 2020; Moghadasia et al., 2020). It had also been shown that ShK-like peptide produced by *Steinernema carpocapsae* is toxic to *Drosophila melanogaster*, and crude venom of *Anthopleura elegantissima* and *S. haddoni* anemones exhibited toxic effects when tested against the rice weevil *Sitophilus oryzae* (Frias et al., 2022; John, 2022). Peptides isolated from *Metridium senile* and *H. crispa* were found to be analgesic (Andreev et al., 2008; Logashina et al., 2017, 2021; Maleeva et al., 2023).

In this study, five representative sea anemone species were collected from the South China Sea and extracted crude venom, which were *Macrodactyla doreensis*, *H. magnifica*, *E. quadricolor*, *S. haddoni*, and *H. crispa*. The biological activity diversity of crude sea anemone venom in hemolytic, enzyme inhibition, anticancer, insecticidal, analgesic and lethal activities was evaluated, aiming to screen the most potential sea anemone resource in the South China Sea and conduct in-depth research to lay the foundation for the development of novel peptide drugs.

2 Results

2.1 Characteristics of sea anemones and component analysis of crude venom

Five species of sea anemones collected from the South China Sea were identified by morphological characteristics as: *M. doreensis* (Quoy and Gaimard, 1833), *H. magnifica* (Quoy and Gaimard, 1833), *E. quadricolor* (Rüppell and Leuckart, 1828), *S. haddoni* (Saville-Kent, 1893), and *H. crispa* (Hemprich and Ehrenberg, 1834) (Figure 1A) (Raghunathan et al., 2014). *M. doreensis* is reddish, with a pronounced and distinctly beige to yellow blotched pedal disc, and fewer tentacles, concentrated on the margin of the oral disc. Morphological characteristics of *H. magnifica* mainly include an ochre-yellow body, reddish-brown pedal disc, column cylindrical, and the tentacles spread over the surface of the oral disc, with purple tips and moderate length of tentacles. *E. quadricolor* is usually light green to green in color, has long, cylindrical and smooth tentacles, which are usually bulbous below the tip with distinctive longitudinal wrinkles, and has a flattened, pinkish oral disc. *S. haddoni* is characterized by a flattened and deeply folded oral disc, extremely short tentacles that are highly robust at periphery of disc, and a beige color with purple spots distributed on the base. *H. crispa* is light ivory, with long, slender and numerous tentacles, partially entwined, whose tips are lavender in color. In addition, five lyophilized extracts of crude venom have different morphologies and show different colors when dissolved in deionized water (Figures 1B, C).

Protein and peptide components were detected by reversed-phase high performance liquid chromatography (RP-HPLC) and SDS-PAGE (Figures 1D, E). RP-HPLC analysis revealed dissimilarities in both peak shapes and peak heights of crude venom. Notably, *H. magnifica* and *H. crispa* exhibited two significant peaks in chromatograms. The proteins in crude venom were mainly distributed at 10-180 kDa in SDS-PAGE analysis. In particular, the common bands at 17 kDa were observed in

H. magnifica, *E. quadricolor*, *S. haddoni* and *H. crispa* and the electrophoretic band of *H. magnifica* was the most abundant.

2.2 Evaluation of the hemolytic and enzyme inhibitory activities

The hemolytic and enzyme inhibitory activities of crude venom were studied using rat erythrocytes and different enzymes, respectively, and the results were shown in Table 1. The hemolysis test showed that crude venom exhibited 100% hemolysis of erythrocytes at concentrations of 1 to 150 µg/mL. Specifically, the venom of *H. magnifica* (1 ± 0.27 µg/mL) and *E. quadricolor* (10 ± 0.27 µg/mL) displayed potent hemolytic activity compared to *S. haddoni* (40 ± 0.27 µg/mL), *H. crispa* (100 ± 1.27 µg/mL) and *M. doreensis* (150 ± 0.53 µg/mL). For enzyme inhibition assay, the trypsin, pepsin and α-galactosidase were selected for the determination of enzyme activities. For trypsin assay, with the exception of *E. quadricolor*, all other venoms were found to inhibit trypsin and *H. magnifica* venom showed the highest inhibitory activity with a value of 251.25 ± 1.43 TIU/mg. Meanwhile, each of crude venom displayed an inhibitory effect on pepsin, the values were in the range of 145.08-391.25 TIU/mg. In contrast, none of these venoms inhibited on α-galactosidase.

2.3 Cytotoxic effects of crude venom on human glioma, hepatocellular carcinoma and lung cancer cells

Due to the rapid growth and poor prognosis of glioma, the invasiveness of hepatocellular carcinoma, the lack of effective treatment, and the high mortality rate of lung cancer, human glioma cells (U251), human hepatocellular carcinoma cells (HepG2) and human lung cancer cells (A549) were selected for cytotoxicity assays and the effects of different concentrations of crude venoms on the viability of the cells was assessed using a cell counting kit (CCK-8) (Ahmad et al., 2024; Dong et al., 2024; Huang et al., 2024; Jin et al., 2024; Lv et al., 2024; Zheng et al., 2024). As shown in Figure 2, cell viability decreased in a concentration-dependent manner with increasing concentrations of crude venom. The order of toxicities of the crude venom extracts were *H. magnifica* > *E. quadricolor* > *S. haddoni* > *M. doreensis* > *H. crispa* for U251, *H. crispa* > *H. magnifica* > *E. quadricolor* > *M. doreensis* > *S. haddoni* for HepG2, and *H. magnifica* > *E. quadricolor* > *S. haddoni* > *M. doreensis* > *H. crispa* for A549. Specifically, the IC_{50} values of *H. magnifica*, *E. quadricolor*, *S. haddoni*, *M. doreensis* and *H. crispa* were 105.0 µg/mL, 108.3 µg/mL, 201.8 µg/mL, 767.9 µg/mL, and 986.4 µg/mL, respectively, for U251 cancer cells (Figure 2F). Strikingly, HepG2 cells showed high sensitivity to crude venom, being most sensitive to *H. crispa* with an IC_{50} value of 10.02 µg/mL and least sensitive to *S. haddoni* with an IC_{50} value of 307.4 µg/mL (Figure 2G). For A549 cells, IC_{50} values of 73.18 µg/mL, 170.9 µg/mL, 179.1 µg/mL, 1858 µg/mL and 2039 µg/mL were observed for *H. magnifica*, *E. quadricolor*, *S. haddoni*, *M. doreensis* and *H. crispa*, respectively (Figure 2H).

2.4 Crude venom exhibit inhibitory effects on migration and invasion of U251 cells *in vitro*

Scratch wound healing and transwell assays were performed to access the effects of crude venom on the migration and invasion of U251 cells. Comparing the migration of U251 cells in the control and treated groups and the invasion images after 24 h of treatment with 100 µg/mL crude venom, it was found that there were reductions in the migration of cells to the scratch site and in the number of invaded cells (Figure 3). As shown in Figure 4, the lowest wound closure rates were observed after 24 h of migration, at

concentrations of 10 µg/mL, 0.2 µg/mL, 1 µg/mL, 0.2 µg/mL, and 10 µg/mL for *M. doreensis*, *H. magnifica*, *E. quadricolor*, *S. haddoni*, and *H. crispa* venoms respectively, the closure rates were 17.67 ± 4.68%, 6 ± 1.53%, 6 ± 1.73%, 11.33 ± 0.67%, and 1.33 ± 2.33%, respectively (Figures 4A–E). *H. magnifica* venom significantly inhibited cell migration, while the venom of *M. doreensis* had the weakest inhibitory effect on migration. In addition, the enhancements of the migration capacity of the cells were observed after 48 h compared to the 24 h. The transwell assay showed that most crude venom inhibited cells invasion in a dose-dependent manner (Figure 4F). Notably, at a concentration of 200 µg/mL, the invasion rates of U251 cells were 18.33 ± 1.76%, 0.33 ±
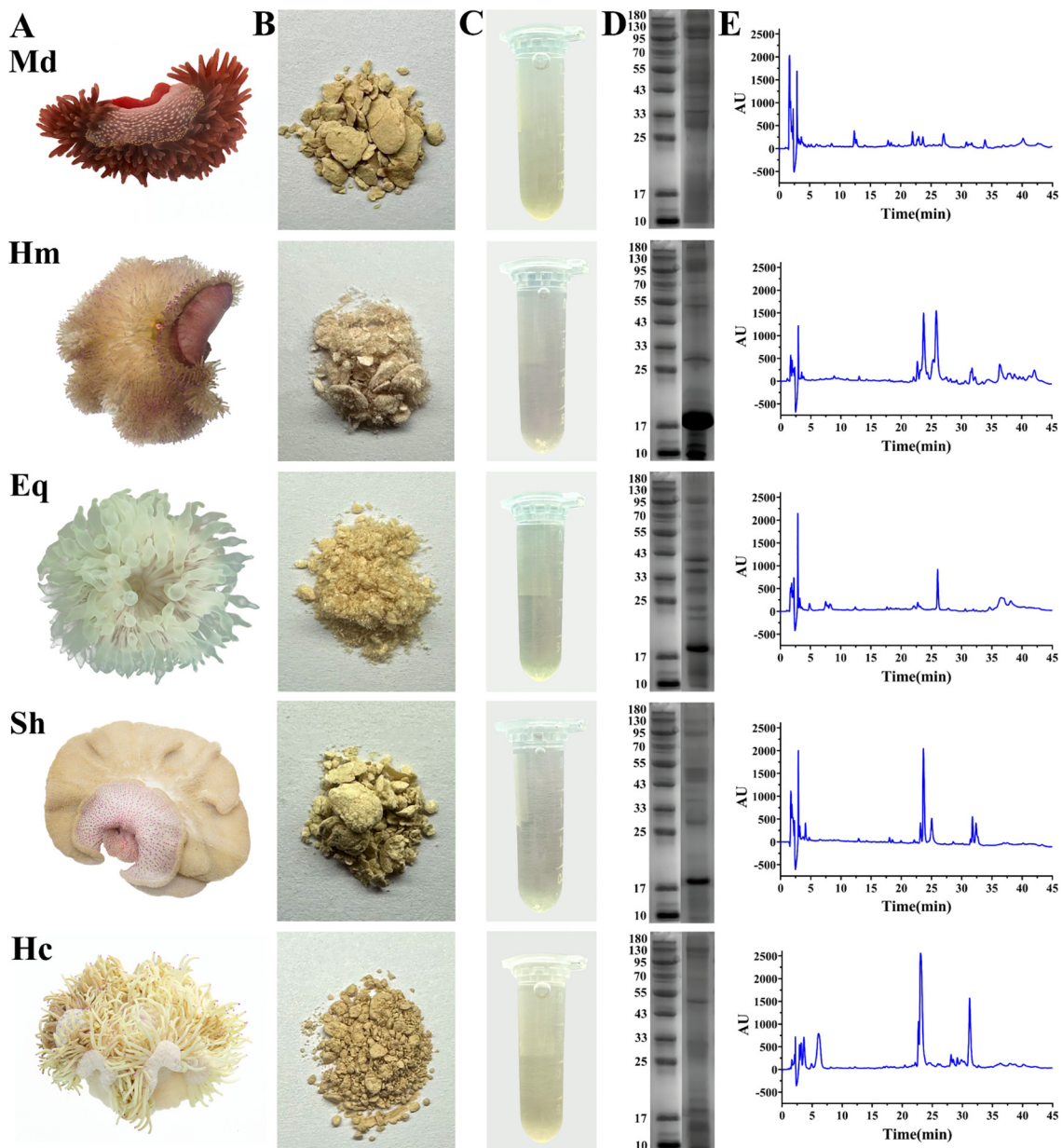
FIGURE 1
Samples of five species of sea anemones and analysis of crude venom using SDS-PAGE and RP-HPLC. **(A)** Macromorphology of five species of sea anemones in the South China Sea. **(B)** Solid forms of crude venom extracted from sea anemones. **(C)** Solutions of crude venom dissolved in deionized water. **(D)** SDS-PAGE analysis of crude venom. **(E)** RP-HPLC analysis of crude venom. Md, *M. doreensis*; Hm, *H magnifica*; Eq, *E quadricolor*; Sh, *S. haddoni*; Hc, *H crispa*.

TABLE 1 The values of hemolysis, trypsin and pepsin inhibition assays for crude venom.

Species	Assay								
	Hemolysis			Trypsin			Pepsin		
	MC$_{100}$	SD	SEM	M	SD	SEM	M	SD	SEM
Macrodactyla doreensis	150.00	0.92	0.53	14.32	0.83	0.48	279.11	3.63	2.09
Heteractis magnifica	1.00	0.47	0.27	251.25	2.48	1.43	145.08	1.91	1.10
Entacmaea quadricolor	10.00	0.46	0.27	Nd	Nd	Nd	161.94	9.42	5.44
Stichodactyla haddoni	40.00	0.47	0.27	133.46	1.07	0.62	391.25	4.09	2.36
Heteractis crispa	100.00	2.20	1.27	22.64	0.78	0.45	250.93	5.02	2.90

MC$_{100}$, the minimum concentration of protein to cause 100% hemolysis of the red blood cells (μg/mL); SD, standard deviation; SEM, standard error of the mean; M, mean (TIU/mg); Nd, not determined.

0.33%, and 24.33 ± 0.33% for *M. doreensis*, *E. quadracolor*, and *H. crispa* venoms, respectively, and the venoms of *H. magnifica* and *S. haddoni* completely suppressed the invasive ability of U251 cells.

2.5 Toxic effects on *Tenebrio molitor* and SF9 cells

Evaluation of the insecticidal activity of crude venom using toxicity assays on *T. molitor* and insect ovarian cells (SF9). The results showed that crude venom significantly reduced the survival of *T. molitor* in a dose- and time-dependent manner (Figures 5A–E), and also reduced the viability of SF9 insect cells in a concentration dependent manner (Figure 5F). After 24 h treatment, *H. magnifica* venom demonstrated the most toxic to *T. molitor* (LD$_{50}$ = 11.44 mg/kg), followed by *E. quadricolor* (LD$_{50}$ = 30.91 mg/kg), *S. haddoni* (LD$_{50}$ = 45.98 mg/kg), *M. doreensis* (LD$_{50}$ = 50.41 mg/kg), and *H. crispa* (LD$_{50}$ = 87.87 mg/kg) venoms. Notably, *H. magnifica* venom resulted in 100% insects mortality at 60 h after 20, 40 and 100 ng/mg treatments, and *E. quadricolor* venom caused all *T. molitor* death within 72 h. In the toxicity assay for SF9 cells, *E. quadricolor* venom showed extremely strong toxicity with an IC$_{50}$ value of about 9.8×10^{-31} μg/mL, the IC$_{50}$ values of *S. haddoni*, *H. crispa*, *M. doreensis* and *H. magnifica* venom on SF9 cells were 39.27 μg/mL, 39.85 μg/mL, 101.2 μg/mL and 110.7 μg/mL, and *H. magnifica* venom was the weakest toxicity to SF9 cells.

2.6 The analgesic effect of crude venom

2.6.1 Assessment of locomotor behavior in larval zebrafish

In order to determine the analgesic properties of crude venom on zebrafish larvae, test was carried out using locomotor behavior. As shown in Figure 6, with the exception of *H. crispa* venom, other venoms gradually reduced the locomotor behavior of larvae with increasing concentrations compared to the acetic acid group. Statistics were conducted on the total distance traveled by zebrafish larvae (Figure 7). Acetic acid group moved a total distance of 6192.67 ± 247.30 mm in 20 min. The total distance of *M. doreensis*, *H. magnifica*, *E. quadricolor*, *S. haddoni*, and *H. crispa*

venoms reached 2767.21 ± 190.44 mm, 2448.82 ± 304.48 mm, 2076.45 ± 195.08 mm, 2867.87 ± 191.91 mm, and 5225.97 ± 626.47 mm at concentrations of 10 μg/ml, 0.5 μg/ml, 2 μg/ml, 2 μg/ml, and 15 μg/ml, respectively (Figures 7A–E), the strongest analgesic effect on zebrafish larvae was observed in *H. magnifica*. However, *H. crispa* was not significantly different from the acetic acid group, indicating no analgesic effect on zebrafish larvae. In addition, after exposure to the crude venom, the four venoms with analgesic effects significantly reduced the distance travelled and remained stable thereafter (Figure 7F).

2.6.2 Hot plate test and crude toxicity lethal test on mice

To assess the analgesic effects of crude venom, a hot plate test was performed. The results were shown in Figure 8. After intraperitoneal injection of 5 mg/kg venoms, crude venom except *H. crispa* venom significantly increased the latency time of mice to lick the hind paws at different times compared to the negative control (Figure 8A). Furthermore, *H. magnifica* venom exhibited the strongest analgesic effect at 90 min, with maximum possible effect (MPE) value of 84.14 ± 8.85%. The strongest analgesic effect of *H. magnifica* venom on zebrafish larvae and mice was selected and injected intraperitoneally into mice at doses of 0.5, 1, 3, 5, 7 and 9 mg/kg. The results showed that after 120 min of injection, the analgesic effect was strongest at 9 mg/kg, with a maximum possible effect value of 55.68 ± 4.54%. The ED$_{50}$ value for the analgesic effect of *H. magnifica* on mice was 8.95 mg/kg (Figure 8B). For lethal assay with *H. magnifica* crude venom, intraperitoneal injection of 11.0 mg/kg of venom was induced 50% lethality of the mice.

3 Discussion

Sea anemones contain complex and abundant venoms that determine the diversity of the biological activities, which provide a broad research space for exploring the biological properties of sea anemones, and also bring great opportunities for the development of safe and efficient novel marine peptide drugs. The sea anemone resources from the South China Sea are abundant and diverse, but traditional methods for isolating and identifying their proteins and peptides are time-consuming and laborious, and their
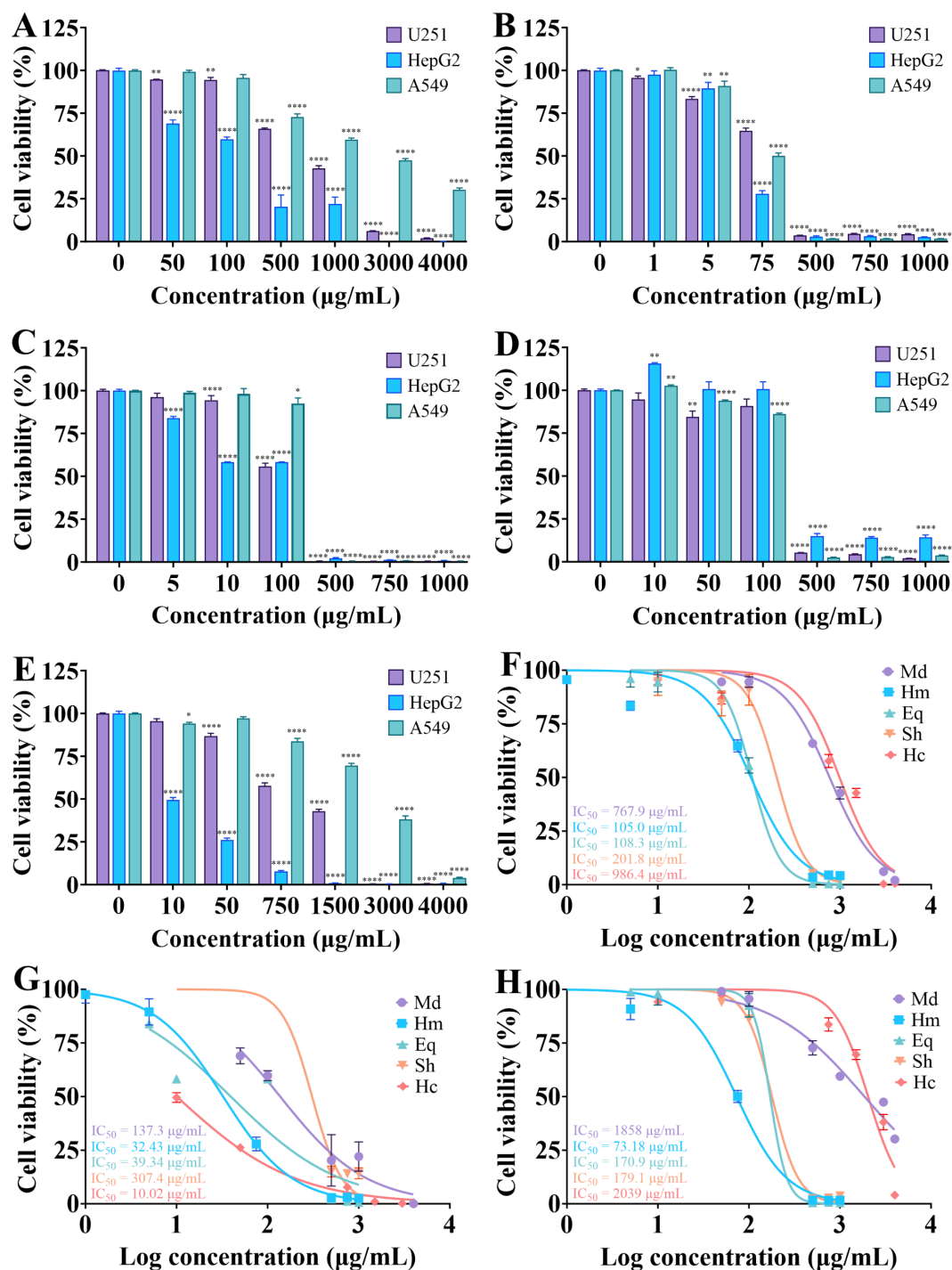
FIGURE 2

Effect of crude venom on the viability of U251, HepG2 and A549 cells. **(A-E)** Results of *M. doreensis*, *H. magnifica*, *E. quadricolor*, *S. haddoni* and *H. crispa* venoms on the cell viability respectively. **(F-H)** Dose effect curves of crude venom on U251, HepG2 and A549 cells, respectively. *P< 0.05, **P< 0.01, ****P< 0.0001 versus the 0 μg/mL group. U251, human glioma cells; HepG2, human hepatocellular carcinoma cells; A549, human lung cancer cells. Md, *M. doreensis*; Hm, *H. magnifica*; Eq, *E. quadricolor*; Sh, *S. haddoni*; Hc, *H. crispa*.

pharmacological activities are complex and varied, making it difficult to obtain effective lead compounds for new drug development. Therefore, this study investigated the crude venom of five representative sea anemones under various activity tracking conditions. Although the pharmacological activity may be caused by multiple components, the best active sea anemone samples were

obtained. For the best pharmacological activity of sea anemones, modern omics technologies such as transcriptomics, proteomics, and metabolomics can be used to systematically explore the protein and peptide groups, and then predict their structure and function through artificial intelligence (AI) driven by deep learning techniques, laying a solid foundation for new drug development.
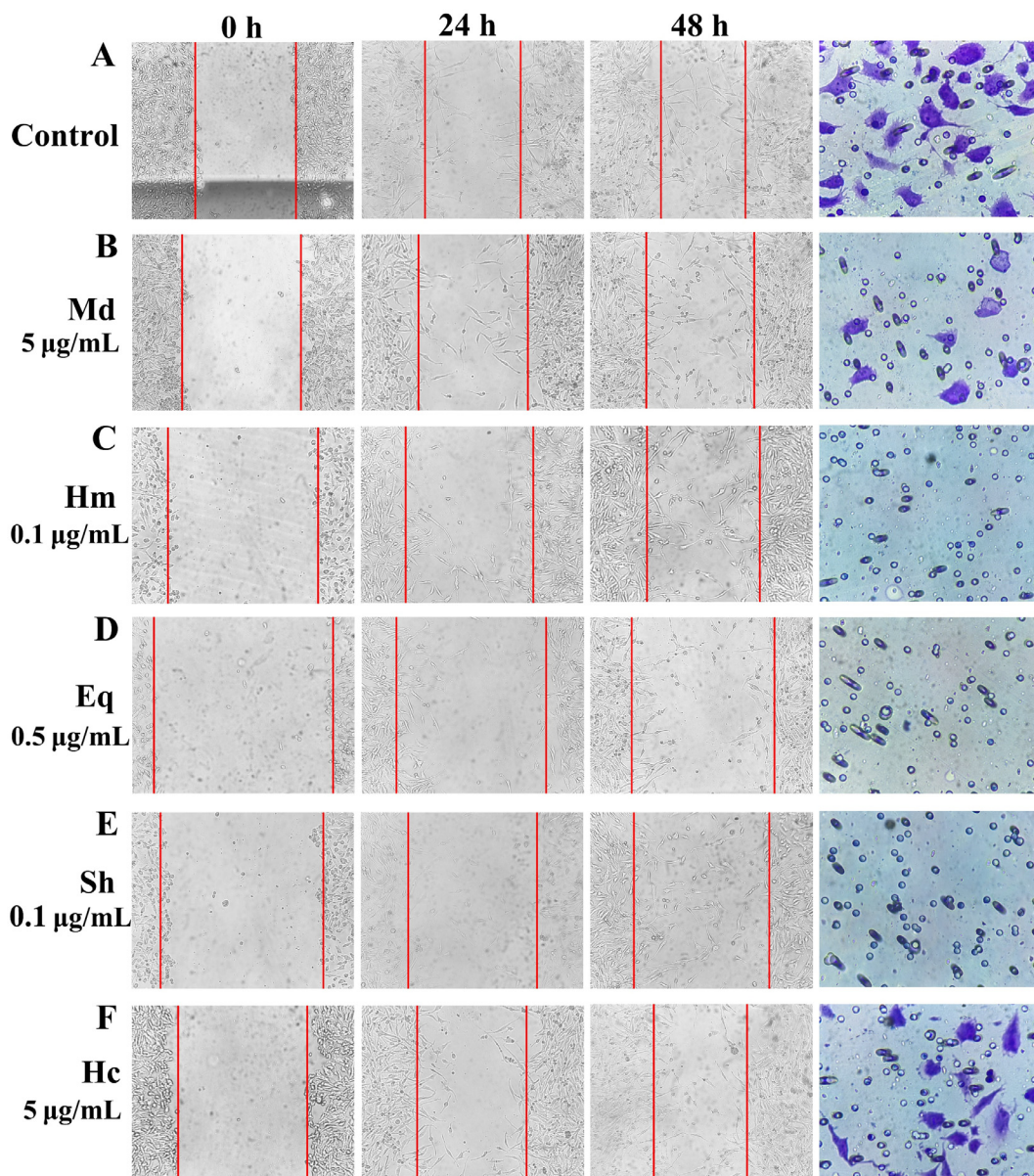
FIGURE 3
The typical images of scratch wound healing and transwell invasion assays for crude venom on U251 cells. **(A)** Pictures of wound healing and transwell invasion assays in the control group. **(B-F)** Pictures of wound healing assay using different concentrations of crude venom and treating U251 cells for 0, 24, 48 h and pictures of transwell assay using 100 µg/mL crude venom for 24 h of U251 cells. Control, control group; Md, *M. doreensis*; Hm, *H magnifica*; Eq, *E quadricolor*; Sh, S. *haddoni*; Hc, *H crispa*.

The protein and peptide fractions in crude venom of five species of sea anemones from the South China Sea were firstly comprehensively analysed using RP-HPLC for the detection of fractions less than 10 kDa in venoms and combined with SDS-PEGE method for detecting a wide range of proteins, and the bioactivities of crude venom were explored using various methods. In the chromatograms, differences in peak shapes and heights of crude venom indicated variations in venom components, and the two distinct peaks of *H. magnifica* and *H. crispa* venoms suggested that the components were extremely high in content. The distributions of crude venom in SDS-PAGE were in the range of 10-180 kDa, which were consistent with the existing studies on

crude venom (Hu et al., 2011; Alcaide et al., 2024). And there was a common band at 17 kDa in four venoms and *H. magnifica* protein band had the highest expression, suggesting that the four venoms may contain the same protein component, which was better represented in *H. magnifica*.

The cytolysins identified in sea anemones can be classified into four groups based on molecular weight and function, one of which was pore-forming proteins or actinoporins (Hoepner et al., 2019; Ramírez-Carreto et al., 2019a). It had been shown that actinoporins and pore-forming proteins had strong hemolytic effects, such as equinatoxin III and FraA, FraB and FraD actinoporins isolated from *Actinia equina* and *Actinia fragacea*, respectively, as well as a pore
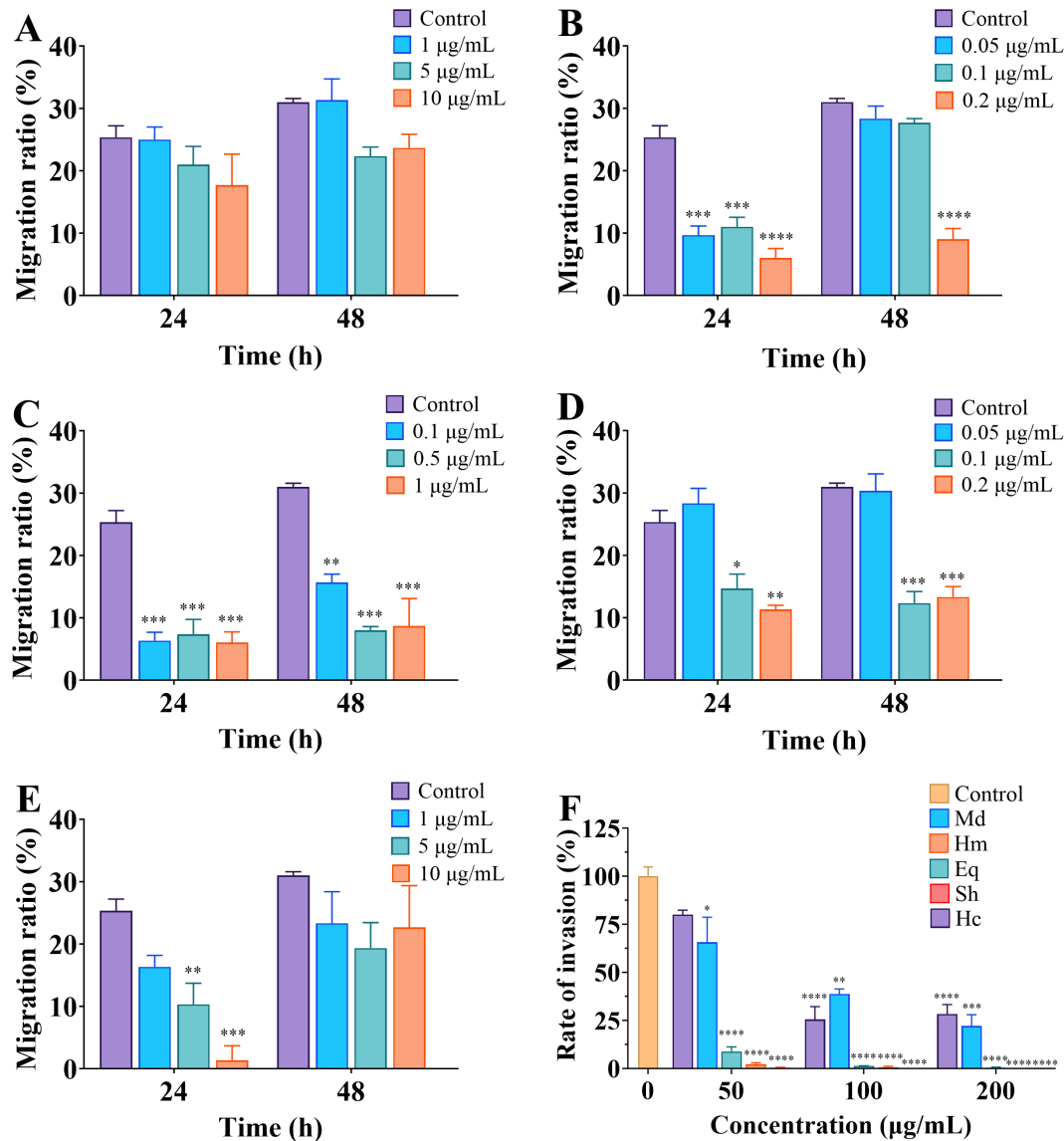
FIGURE 4
Crude venom suppress migration and invasion of U251 cells. **(A-E)** The migration ratios of cells at 24 h and 48 h after treatment of *M. doreensis*, *H. magnifica*, *E. quadricolor*, *S. haddoni* and *H. crispa* venoms, respectively. **(F)** Invasion rates of crude venom on U251 cells at 50, 100 and 200 μg/mL concentrations. Md, *M. doreensis*; Hm, *H. magnifica*; Eq, *E. quadricolor*; Sh, *S. haddoni*; Hc, *H. crispa*. *p<0.05, **p<0.01, ***p<0.001, **** p<0.00001 versus control group.

forming toxin called sticholysin II extracted from *Stichodactyla helianthus*, had strong hemolytic activity (Suput et al., 2001; Celedon et al., 2013; Morante et al., 2019). This hemolysis mainly occurs through the binding of toxins to the cell membrane, oligomerization of the protein, followed by translocation of the N-terminal α-helix through the lipid bilayer leading to the formation of functional pores in the plasma membrane of the erythrocytes (Valle et al., 2018; Morante et al., 2019). In this study, all crude venom extracts showed hemolytic activity, indicating that the hemolytic properties of venoms may be related to the presence of pore-forming proteins or actinoporins. And the hemolytic activities of *H. magnifica*, *S. haddoni* and *H. crispa* had been reported to be 3.6×10^4, 56.3 and 3.3×10^4 HU/mg, respectively (Khoo et al., 1993; Subramanian et al., 2011; Leychenko et al., 2018).

The differences in these values compared to the hemolytic activity of the same species collected in the South China Sea may be related to the diversity of the environments in which the species live (Monastyrnaya et al., 2010).

Protease inhibitors are a group of peptides and proteins with potential applications in cardiovascular, inflammatory and even immune diseases based on the control of proteolysis (Ramirez-Carreto et al., 2019b). At present, several peptides with protease inhibitory activity have been extracted from sea anemones. The main function of most known Kunitz-type peptides is protease inhibition, especially trypsin, and their structure enables the formation of two loops responsible for protease inhibition (Kvetkina et al., 2022; Mazzi Esquinca et al., 2023). HCIQ2c1, HCIQ4c7, and HMIQ3c1 of Kunitz-type peptides had been found
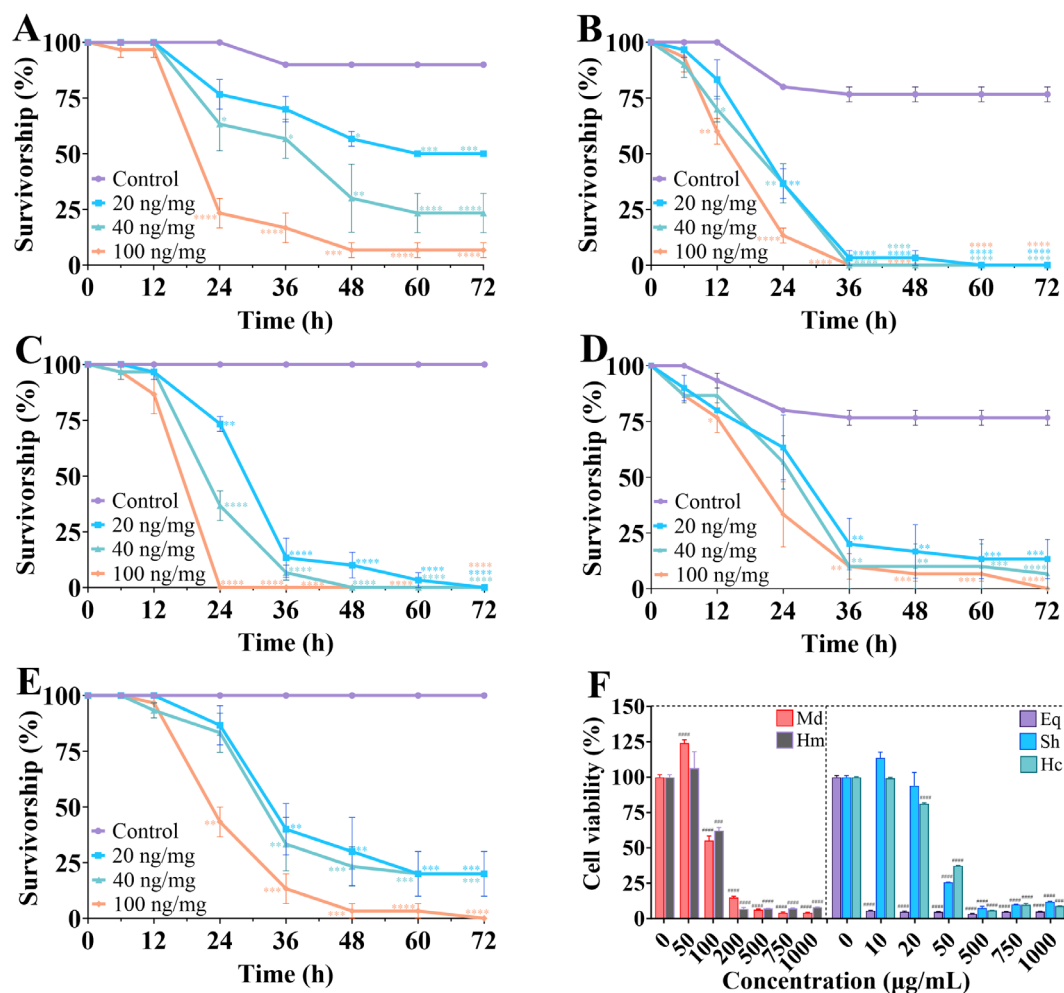
FIGURE 5
Survival of crude venom in insecticidal experiments on *T. molitor* and SF9 cells. **(A-E)** Determination of the toxicity of crude venom of *M. doreensis*, *H. magnifica*, *E. quadricolor*, *S. haddoni* and *H. crispa* at different times to *T. molitor*, respectively. **(F)** The cell viability of SF9 cells for five venoms at different concentrations in CCK-8 assay. Md, *M. doreensis*; Hm, *H. magnifica*; Eq, *E. quadricolor*; Sh, *S. haddoni*; Hc, *H. crispa*. *P< 0.05, **P< 0.01, ***p<0.001, ****P< 0.0001 versus control group; ###P< 0.001, ####P< 0.0001 versus the 0 µg/mL group, n = 100.

to interact with several serine proteases (Kvetkina et al., 2022). In the present study, the specific inhibitory effect of sea anemone venoms on different proteases speculates that Kunitz-type peptides may be present in the crude venom, which provides a basis for further studies on the isolation of Kunitz-type peptides with pharmacological effects from these venoms.

Nowadays, Hmg 1b-2 and Hmg 1b-4 peptides from *H. magnifica* at 0.1-1 mg/kg have significant anti-inflammatory effects (Gladkikh et al., 2023). For the anticancer activity of South China Sea anemones, it was found that each of crude venom was cytotoxic to U251, HepG2, and A549 cancer cells, this result enhances the values of sea anemones in anticancer research and highlights the promising future of sea anemone toxin research, and transcriptomics will be used to sequence the cells treated with crude venom to verify the key targets of inhibitory effect on these cancer cells. However, preliminary studies have also detected cytotoxic activity of crude venom against normal cells, and it is hoped that after the isolation of specific peptide toxins, peptide toxins with specific inhibitory activity on cancer cells and low toxicity on

normal cells can be screened out. Currently, glioma is the most common malignant brain tumor with high mortality and poor outcome, and is considered one of the most intractable early-death solid tumor to treat in neurosurgery (Anton et al., 2012; Guo et al., 2022). The drugs available today for the treatment of glioma are cisplatin, lomustine and temozolomide, but gliomas greatly limit the efficacy of treatment due to resistance to these drugs (Ren et al., 2014). Therefore, in this study, the inhibitory effect of crude venom from five sea anemones on the migration and invasion of U251 cells was verified by scratch wound healing and transwell invasion assays, so the peptide drugs of five sea anemones from the South China Sea may be an important source for use in the treatment of gliomas. And more significant migration inhibition was observed at 24 h than at 48 h in the migration assay, which may be attributed to the continued proliferation of surviving cells after 24 h. The cytotoxicity, invasion and migration assays of the crude venom from sea anemones have confirmed the potential presence of anticancer peptides in sea anemones, which require solid phase peptide synthesis (SPPS), RP-HPLC purification and activity
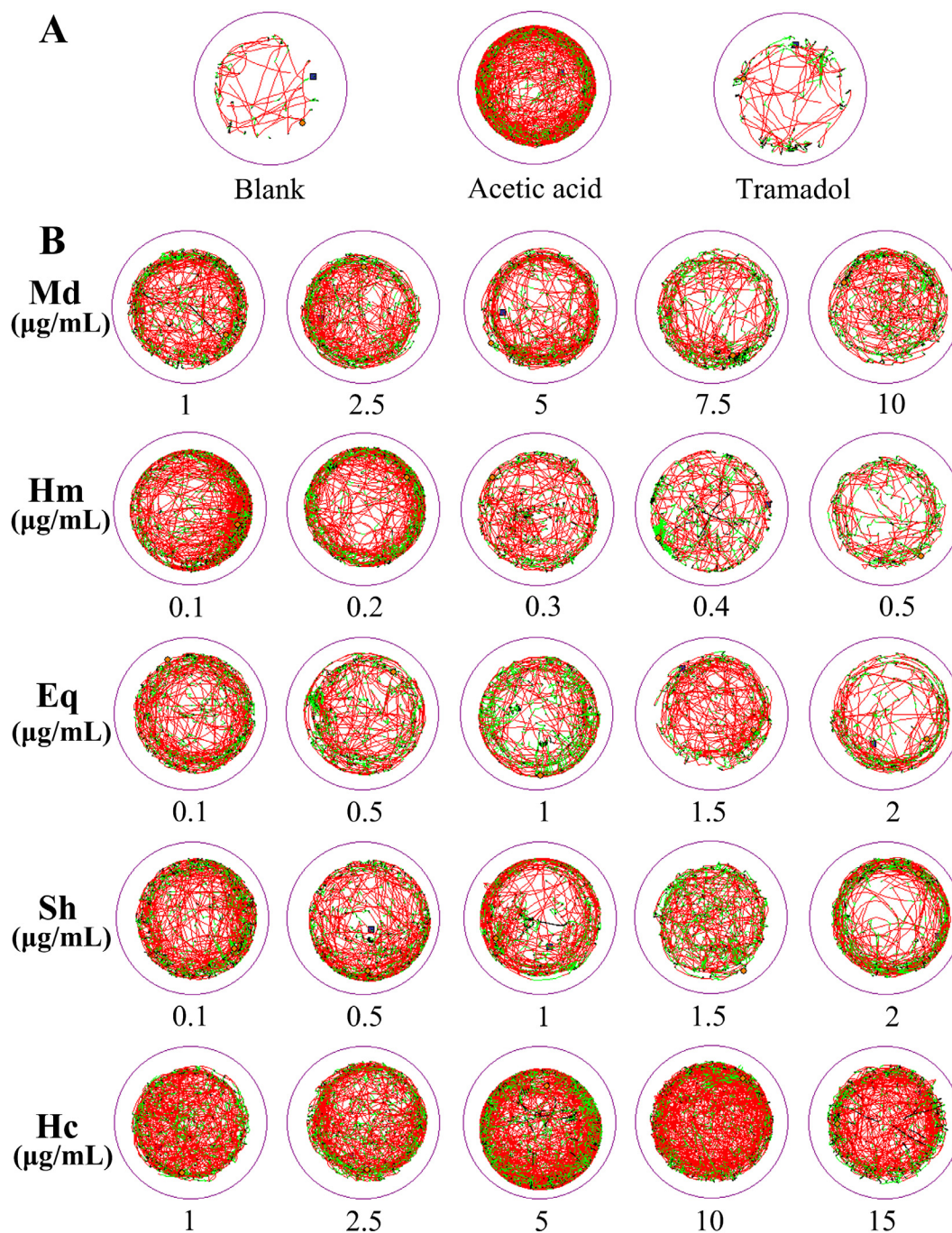
FIGURE 6
Locomotor behavior of zebrafish larvae after crude venom treatment. **(A)** Behavioral trajectories of zebrafish larvae in blank, acetic acid and tramadol groups. **(B)** Behavior of zebrafish larvae in different concentrations of crude venom. Motion trajectory was recorded every 5 s and represented as a curve. Detected instantaneous velocity and displayed in different colors (black,< 2 mm/s; green, 2-8 mm/s; red, > 8 mm/s). Md, *M. doreensis*; Hm, *H magnifica*; Eq, *E quadricolor*; Sh, *S. haddoni*; Hc, *H crispa*.

verification. This provides a new way to develop novel and efficient anticancer peptide drugs from South China Sea anemones.

Sea anemone venoms were the main research targets for the development of insecticidal peptides of biotoxin origin (Yan et al., 2013). The most common insecticide currently mainly act on the insect nervous system, with common targets being Nav and Kv channels, glutamate and nicotinic acetylcholine receptors (Windley et al., 2012; Ren et al., 2018). *Bunodosoma granulifera* and *H. crispa*

have been reported to affect Nav channels and can act as insecticides (Bosmans et al., 2002; Kalina et al., 2020). In this study, crude venom showed excellent insecticidal activity against *T. molitor* and SF9 cells, peptides that act on Nav channels may be present in crude venom. However, it was noted that *E. quadricolor* showed extreme toxicity on SF9 cells, while *H. magnifica* was the most toxic to *T. molitor*, suggesting that in addition to evaluations at the cellular level, insect experiments are needed to validate these results in order
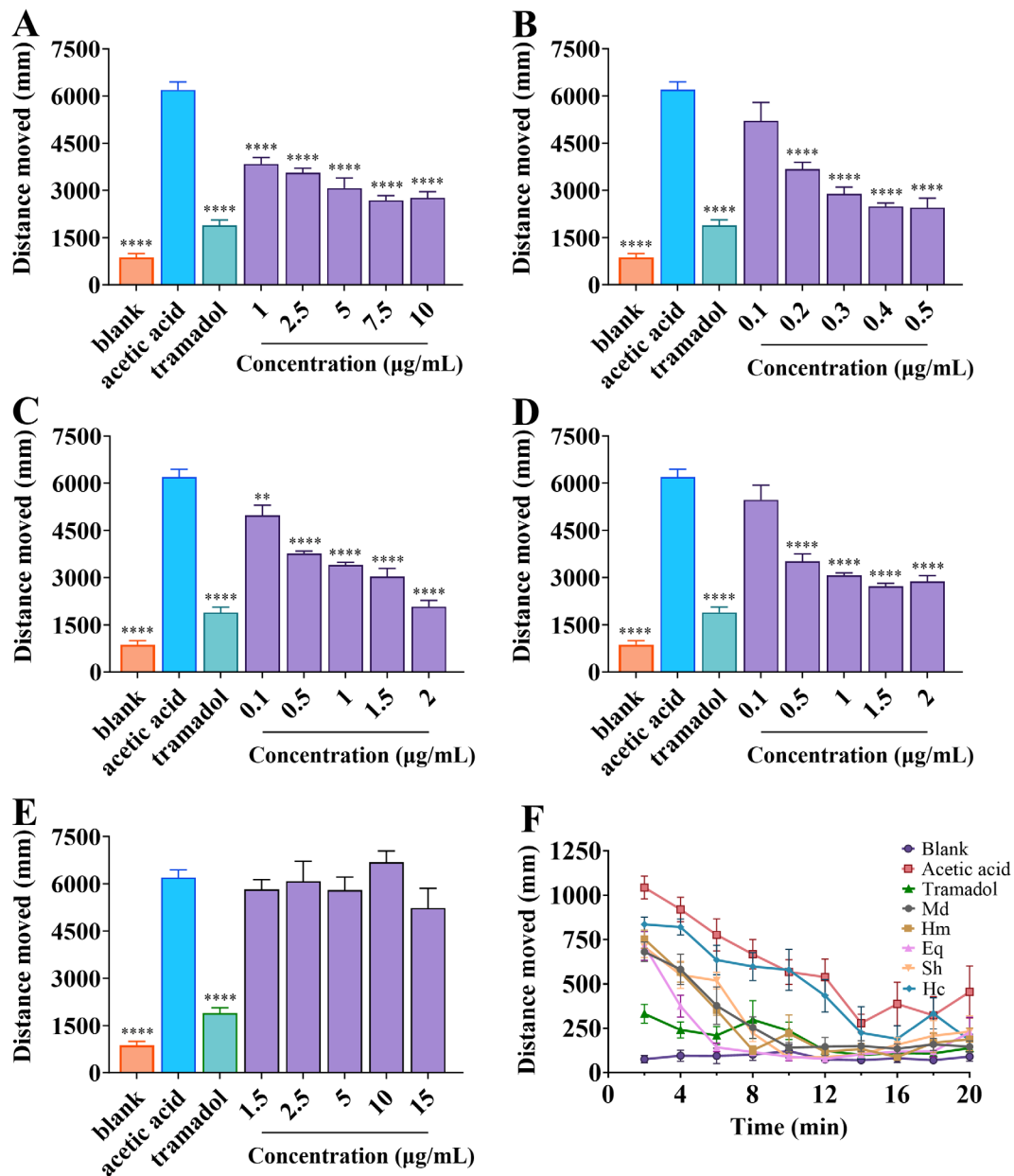
FIGURE 7

Distance travelled by zebrafish larvae in different treatment groups. **(A-E)** Total distance travelled by zebrafish larvae within 20 min after exposure to *M. doreensis*, *H. magnifica*, *E. quadricolor*, *S. haddoni* and *H. crispa*, respectively. **(F)** The variation of travel distance over time for zebrafish larvae juveniles of different treatment groups within 20 min. Md, *M. doreensis*; Hm, *H. magnifica*; Eq, *E. quadricolor*; Sh, *S. haddoni*; Hc, *H. crispa*. **P< 0.01, ****P< 0.0001 versus acetic acid group, n = 6.

to gain a comprehensive understanding of the effects of anemone toxins in insects. These results further validate the potential of natural biotoxins for insecticidal activity and allow further study of toxin peptides in crude venom for the development of new insecticidal peptide lead molecules.

M. doreensis, *H. magnifica*, *E. quadricolor*, and *S. haddoni* venoms were found to have analgesic effects on zebrafish larvae and mice in locomotor behavior and hot plate tests, which supported earlier findings on crude extracts of some echinoderms (Kanagarajan et al., 2008). Zebrafish, sharing approximately 70% homology with human genes, is now an ideal model system for drug

and gene discovery and is becoming increasingly popular in the direction of understanding the pharmacology of drugs, especially toxicity and behavioral effects (Howe et al., 2013; Kirla et al., 2021). Acetic acid was used as a model in behavioral experiments with zebrafish larvae, which was added to water to cause pain as a nociceptive stimulus. Combined with the hot plate test, the results of this study found that *H. magnifica* venom had the best analgesic effect on zebrafish and mice. At present, a variety of peptides with analgesic effects have been found in *H. crispa*, such as HCRG21 and APETx2, and the analgesic mechanisms of sea anemone peptides were mainly classified as full antagonist of TRPV1 receptor and
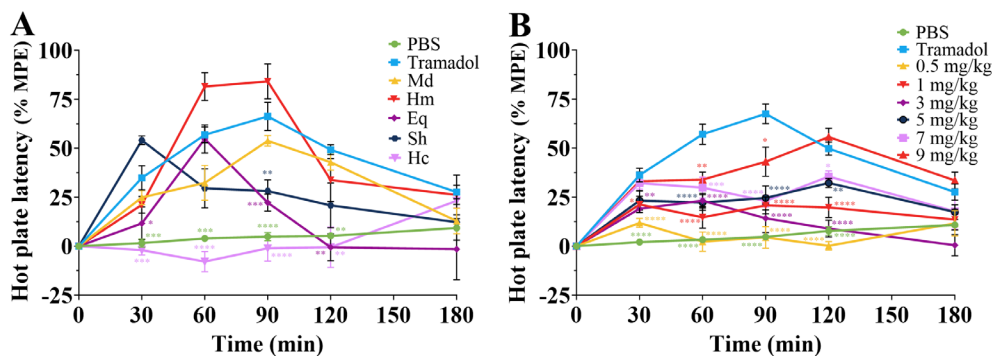
FIGURE 8
Analgesic effects of crude venom and PBS negative and tramadol positive controls in mice. **(A)** The MPE of pain reaction in mice to injection of crude venom at 5 mg/kg. **(B)** The MPE of *H magnifica* venom at different doses on analgesic in mice. Md, *M. doreensis*; Hm, *H magnifica*; Eq, *E quadricolor*; Sh, *S. haddoni*; Hc, *H crispa*. *P< 0.05, **P< 0.01, ***P< 0.001, ****P< 0.0001 versus the PBS group, n = 6.

selective blocker of the proton-sensitive channel acid-sensing ion channel 3 (ASIC3) (Deval et al., 2008; Monastyrnaya et al., 2016; Logashina et al., 2021). In this study, sea anemones collected from the South China Sea demonstrated the strongest analgesic activity of *H. magnifica*, whereas *H. crispa* crude venom had no analgesic activity. It can be assumed that the different peptides of these anemones lead to different inhibitory mechanisms involved or no inhibitory effect, it is necessary to strengthen the study of peptides with analgesic effects in *H. magnifica* from the South China Sea and to use patch-clamp to record the targets that produce analgesic effects (Salvage et al., 2023; Zhang et al., 2023), in order to develop safe and efficient analgesic drugs with few side effects.

4 Materials and methods

4.1 Samples collection and crude venom preparation

The species of five sea anemones used in this study were collected from the South China Sea (18°N, 112°E) at a depth of 4 m in March 2023. Later, these sea anemones were grown in glass aquariums filled with seawater. Following 1 to 2 weeks of maintenance, crude venom extracts were obtained from fresh samples adoption a homogenization method, which primarily requires mincing and homogenizing sea anemones and then freezing at 4°C, followed by centrifugation of the samples at 10000 rpm for 30 min and lyophilized. Then, the lyophilized samples were dissolved and centrifuged, the supernatant was desalted using dialysis, finally crude venom of sea anemones were obtained through freeze-drying.

4.2 The reverse-phase HPLC

Preliminary detection of crude venom fractions was performed by using RP-HPLC with a UV detector and C18 column (Diamonsil, 250 × 4.6 mm, 5 μm). 10 mg of each crude venom was weighed and dissolved in 1 mL of deionized water, and then

centrifuged at 4°C and 10000 rpm for 10 min. The supernatant was filtered through a 0.45 μm microporous filtration membrane, and then 100 μL sample was injected into the RP-HPLC system with the aid of the auto-sample. The mobile phase used in this study A (0.1% trifluoroacetic acid (TFA) acetonitrile solution) and B (0.1% TFA ultra-pure water). Before use, the mobile phase solvents were filtered through 0.45 μm filter papers and degassed for 15 min on an ultrasonicator. Separation at a constant flow rate of 1 mL/min for 65 min using a linear gradient (5-70% A) and monitored by absorbance at 214 nm.

4.3 SDS-PAGE analysis

SDS-PAGE was performed essentially as described by Laemmli (Laemmli, 1970). 10 mg of each crude venom was weighed and dissolved in 1 mL of deionized water, and then centrifuged at 1000 rpm for 5 min. 16 μL of the supernatant was mixed with 4 μL of the sample loading buffer (0.01 M Tris-HCl, 10% (w/v) SDS, 10% (v/v) glycerol, 0.1% (w/v) bromophenol blue, 2% β-mercaptoethanol) and then boiled for 10 min. Samples were loaded onto gel slab consisting of 12% separating gel (pH 8.8) and 4% stacking gel (pH 6.8), and subjected to electrophoresis at 100 V for 1 h. The electrophoresis gels were stained using Coomassie Brilliant Blue R-250.

4.4 Hemolytic activity assay

Hemolysis, as indicative of red blood cells (RBCs) membrane destruction caused by interaction with substances, was evaluated by measuring the released hemoglobin (Macczak et al., 2015; Almasi et al., 2019). Hemolytic activity of crude venom was determined according to the method of Zhang with minor modifications (Zhang et al., 2010). Briefly, harvested rat blood samples were collected in tubes containing heparin to prevent coagulation and centrifuged at 1500 rpm for 10 min at 4°C. Then, the RBCs at the bottom were collected and washed three times with PBS at PH7.4 and the RBCs were resuspended in saline to a final concentration of 1% (v/v). Crude venom solutions dissolved in deionized water were

mixed with RBCs and incubated at 37°C for 1 h before centrifugation at 1500 rpm for 10 min at 4°C. 100 µL of the supernatants were pipetted into 96-well microtiter plate and the absorbance was measured at 540 nm using a microplate reader (Synergy HTX, Bio-Tek, USA). RBCs were treated with deionized water for fully hemolytic and used as positive controls. Percent hemolysis was calculated using the following formula:

$$\textbf{percent hemolysis} = [\textbf{OD540 (samples)} / \textbf{OD540 (positive control)}] \times \textbf{100}\%$$

4.5 Trypsin inhibitory activity

N-α-benzoyl-D, L-arginine p-nitroaniline hydrochloride (BAPNA) was a chromogenic substrate for trypsin, which hydrolyses BAPNA to produce p-nitroaniline, and the absorbance of the solution is measured at 410 nm (Erturk et al., 2016). Trypsin inhibitory activity of crude venom was determined as per the method of Erlanger using BAPNA as a substrate in Tris-HCl buffer (pH 8.2, containing 0.1 M CaCl$_2$) (Erlanger et al., 1961). Each crude venom dissolved in deionized water was mixed with the substrate and incubated at 37°C for 10 min, the reaction was then terminated by the addition of 30% (v/v) acetic acid (100 µL). Finally, substrate hydrolysis was determined at 410 nm. One unit of trypsin activity can be defined as a 0.01 unit increase in absorbance at 410 nm and trypsin inhibitory activity was defined as inhibiting one unit of trypsin activity.

4.6 Pepsin inhibitory activity

Hemoglobin can be rapidly hydrolyzed by pepsin and the inhibitory effect of pepsin was determined using bovine hemoglobin as a substrate (Marks et al., 1973; Vaghefi et al., 2002). Pepsin inhibition assay was performed using a mixture of pepsin, hemoglobin and crude venom followed by incubation at 37°C for 10 min before the reaction was stopped by the addition of 100 µL of 30% trichloroacetic acid. After centrifugation at 10000 rpm for 10 min, the supernatants were pipetted into cuvettes and absorbances were read at 660 nm.

4.7 Inhibitory activity assay of α-galactosidase

α-Galactosidase interacted with p-nitrophenyl-α-D-galactopyranoside (PNPG) to produce p-nitrophenol, which absorbed at 405 nm (Sakharayapatna Ranganatha et al., 2021). To determine the inhibitory activity of crude venom against α-galactosidase using PNPG as substrate. The enzyme and crude venom solutions were mixed in 0.1 M phosphate buffer and reactions were incubated at 37°C for 30 min, then the substrate was added. Finally, the reactions were terminated by the addition of 1 M Na$_2$CO$_3$ and absorbances at 405 nm were finally measured.

4.8 Cell cultures

Cancer cell lines used in this study included insect cells (SF9), human glioma cells (U251), human hepatocellular carcinoma cells (HepG2) and human lung cancer cells (A549), and were obtained from Hainan Provincial Key Laboratory of Carcinogensis and Intervention. SF9 insect cells were seeded in cell culture flasks and cultured in SFM medium supplemented with 10% fetal bovine serum (FBS) at 27°C, other cells were incubated in DMEM medium supplemented with 10% FBS at 37°C and 5% CO$_2$ for the CCK-8 assay, wound healing and transwell invasion assays. Then, the spent medium was removed, control wells received fresh medium without crude venom, and treatment wells received medium with different concentrations of crude venom.

4.9 CCK-8 assay

10 mg of each crude venom was weighed and dissolved in the culture medium, then the crude venom solution was taken for dilution. U251, HepG2, A549 and SF9 cells were seeded into 96-well cell culture plates at a density of 1×10^4 cells/well and treated U251, HepG2 and A549 cells with differing concentrations of *M. doreensis* (50, 100, 500, 1000, 3000, 4000 µg/mL), *H. magnifica* (1, 5, 75, 500, 750, 1000 µg/mL), *E. quadricolor* (5, 10, 100, 500, 750, 1000 µg/mL), *S. haddoni* (10, 50, 100, 500, 750, 1000 µg/mL), and *H. crispa* (10, 50, 750, 1500, 3000 and 4000 µg/mL) venoms for 24 h, the *E. quadricolor*, *S. haddoni* and *H. crispa* venoms were formulated into 10, 20, 50, 500, 750, and 1000 µg/mL and solutions of 50, 100, 200, 500, 750 and 1000 µg/mL were prepared using *M. doreensis* and *H. magnifica* venoms to treat SF9 cells. Following treatment, 10 µL of CCK-8 solution was added to each well and then the culture was continued incubation for 2 h at 37°C. Absorbance values at 450 nm were measured using the microplate reader.

4.10 *In vitro* wound healing study

Assessment of the migratory ability of U251 cells using the wound healing assay. Cells were inoculated in 24-well plates at a density of 1×10^5 cells/well, cultured for 24 h, and then scraped perpendicular to the bottom of the wells with a 200 µL sterile pipette tip. Following this, the cellular debris were washed twice with PBS, and serum-free medium containing different concentrations of crude venom were incubated for 48 h at 37°C in a 5% CO$_2$ incubator, using untreated cells as controls. Images were taken after 0 h, 24 h, and 48 h under an inverted microscope (magnification × 100) and measurements of wound area were performed using ImageJ software. The reduction of wound-size was calculated according to the following formula:

$$\textbf{wound} - \textbf{size reduction}\,(\%) = [(\textbf{original scratch area} - \textbf{the point scratch area}) / \textbf{original scratch area}] \times \textbf{100}\%$$

4.11 Transwell invasion assay

For transwell invasion assay, diluted matrigel (1:8) was applied to the chambers of the transwell apparatus and these chambers were incubated for 1 h at 37°C. A total of 5×10^4 U251 cells containing 50, 100 and 200 µg/mL of crude venom were evenly seeded in the upper chamber of the transwell, using cells untreated with crude venom as a control, and DMEM medium with 10% FBS was placed in the lower chamber. After incubation at 37°C for 24 h, U251 cells were fixed with 4% paraformaldehyde for 30 min and then stained with 0.1% crystal violet for 30 min and observed under a microscope (magnification × 400) and counted using ImageJ.

4.12 Toxicity assay on *Tenebrio molitor*

Each crude venom was dissolved with saline and formulated into concentrations of 20, 40 and 100 ng/mg for assessing the toxicity of the venom to *T. molitor*. Three replicate groups of *T. molitor* were injected of per dose, and the number of survivor insects were counted after 6, 12, 24, 36, 48, 60 and 72 h of application. Then the survival rates of *T. molitor* were determined after the addition of venoms. Control groups were applied with saline.

4.13 Evaluation of the analgesic activity

4.13.1 Locomotor behavior of zebrafish larval

Zebrafish, which share a high genetic similarity with mammals and possess a complex nervous system that allows for assessment of the swimming response to nociceptive stimuli, were utilized as a model to analyze pain responses by measuring total distance in locomotor behavior (Park et al., 2021; Zaig et al., 2021). 10 mg of each crude venom was weighed and dissolved in deionized water, then the crude venom solution was taken for dilution. Zebrafish larvae at 5-day post-fertilization (5-dpf) were introduced into the wells of 24-well plates (1 larva per well), given 1 mL of different concentrations of crude venom and observed for 20 min, using 6 zebrafish larvae for each concentration. Then 1 mL of acetic acid was added to each well and placed in a zebrafish tracking system (Viewpoint Life Sciences, Montreal, QC, Canada) for 20 min. Each larva was recorded 10 times (2 min each) and the total distances swum by the larva were finally recorded. An acetic acid group was add to the water as a nociceptive stimulus to cause pain and 15 µg/mL tramadol was used as a positive control to evaluate its analgesic effect. The blank group did not ingest acetic acid, both the acetic acid group and the experimental group ingested equal amounts of acetic acid.

4.13.2 Hot plate test

The hot plate test was used to assess central antinociceptive activity in mice, indicating the antinociceptive effect (Benmaarouf et al., 2020; Vandeputte et al., 2022). Mice were placed on a hot plate (maintained at 55 ± 0.5°C) and the time of licking the hind paws were recorded within 60 s to prevent tissue damage. Selected animals were injected intraperitoneally with a dose of 5 mg/kg crude venom dissolved using saline. And pain thresholds were assessed at 30, 60, 90, 120 and 180 min deescalation after treatment. The negative control group by intraperitoneal injection of PBS, with a dose of 50 mg/kg of tramadol as a positive control. The analgesic effects of crude venom were quantified as a percentage of the maximum possible effect (%MPE) to equalize the bases latency time in different animals using the following formula:

$$\% \text{ MPE} = [(\text{test latency} - \text{basal latency}) / (\text{cutoff time} - \text{basal latency})] \times 100\%$$

4.14 Determination of lethality in mice

High concentrations of *H. magnifica* crude venom were found to cause rapid death in mice by hot plate test. Specifically, the mice were divided into five groups and given 8.9 mg/kg, 9.8 mg/kg, 10.8 mg/kg, 11.8 mg/kg and 13.0 mg/kg of *H. magnifica* venom, deaths were recorded after intraperitoneal injection of venom and the LD_{50} value was calculated using the trimmed Spearman-Karber method.

4.15 Statistical analysis

All experiments were performed in triplicate, plotted and statistically analysed using Adobe Photoshop 20.0.4, GraphPad Prism 10.1.2 and SPSS 19.0 software. Results were presented as mean ± SEM and analysed using one-way ANOVA, with $P < 0.05$ considered statistically significant.

5 Conclusions

In summary, studies on crude venom extracted from five types of South China Sea anemones, including *M. doreensis*, *H. magnifica*, *E. quadricolor*, *S. haddoni*, and *H. crispa*, have shown that the successfully screened *H. magnifica* exhibits extremely strong biological activity, mainly manifested in hemolysis, enzyme inhibition, anticancer, insecticidal, and analgesic activities. Especially, the crude venom of *H. magnifica* has been extensively studied on U251 cells, and it has been found that the crude venom can significantly inhibit the migration and invasion of U251 cells at low concentrations. Therefore, sea anemone *H. magnifica* has been identified as one of the highly promising and efficient therapeutic drugs in the South China Sea, which requires the development of novel anticancer and analgesic peptide drugs through sequencing technology and subsequent peptide synthesis work to promote the treatment of human diseases.

Data availability statement

The original contributions presented in the study are included in the article/supplementary material. Further inquiries can be directed to the corresponding authors.

Ethics statement

Ethical approval was not required for the studies on humans in accordance with the local legislation and institutional requirements because only commercially available established cell lines were used. The animal study was approved by the Ethics Committee of Hainan Medical University. The study was conducted in accordance with the local legislation and institutional requirements.

Author contributions

PH: Writing – original draft, Methodology, Formal analysis, Data curation. ML: Writing – original draft, Methodology, Data curation. JF: Writing – review & editing. YL: Writing – review & editing. BY: Writing – review & editing, Conceptualization. BG: Writing – review & editing, Funding acquisition, Conceptualization.

Funding

Acknowledgments

Conflict of interest

The authors declare that the research was conducted in the absence of any commercial or financial relationships that could be construed as a potential conflict of interest.

Publisher's note

All claims expressed in this article are solely those of the authors and do not necessarily represent those of their affiliated organizations, or those of the publisher, the editors and the reviewers. Any product that may be evaluated in this article, or claim that may be made by its manufacturer, is not guaranteed or endorsed by the publisher.

References

Ahmad, N., Chen, L., Yuan, Z., Ma, X., Yang, X., Wang, Y., et al. (2024). Pyrimidine compounds BY4003 and BY4008 inhibit glioblastoma cells growth via modulating JAK3/STAT3 signaling pathway. *Neurotherapeutics* 21, e00431. doi: 10.1016/j.neurot.2024.e00431

Alcaide, M., Moutinho Cabral, I., Carvalho, L., Mendes, V. M., Alves de Matos, A. P., Manadas, B., et al. (2024). A comparative analysis of the venom system between two morphotypes of the sea anemone *actinia equina*. *Animals* 14, 981. doi: 10.3390/ani14060981

Almasi, T., Jabbari, K., Gholipour, N., Mokhtari Kheirabadi, A., Beiki, D., Shahrokhi, P., et al. (2019). Synthesis, characterization, and *in vitro* and *in vivo* (68)Ga radiolabeling of thiosemicarbazone Schiff base derived from dialdehyde dextran as a promising blood pool imaging agent. *Int. J. Biol. Macromol.* 125, 915–921. doi: 10.1016/j.ijbiomac.2018.12.133

Andreev, Y. A., Kozlov, S. A., Koshelev, S. G., Ivanova, E. A., Monastyrnaya, M. M., Kozlovskaya, E. P., et al. (2008). Analgesic compound from sea anemone *Heteractis crispa* is the first polypeptide inhibitor of vanilloid receptor 1 (TRPV1). *J. Biol. Chem.* 283, 23914–23921. doi: 10.1074/jbc.M800776200

Anton, K., Baehring, J. M., and Mayer, T. (2012). Glioblastoma multiforme. *Hematology/Oncol. Clinics North America* 26, 825–853. doi: 10.1016/j.hoc.2012.04.006

Ashwood, L. M., Undheim, E. A. B., Madio, B., Hamilton, B. R., Daly, M., Hurwood, D. A., et al. (2022). Venoms for all occasions: The functional toxin profiles of different anatomical regions in sea anemones are related to their ecological function. *Mol. Ecol.* 31, 866–883. doi: 10.1111/mec.16286

Benmaarouf, D. K., Pinto, D. C. G. A., China, B., Zenia, S., Bendesari, K. B., and Ben-Mahdi, M. H. (2020). Chemical analysis, antioxidant, anti-inflammatory and antinociceptive effects of acetone extract of Algerian *solenostemma argel* (Delile) hayne leaves. *Int. J. Curr. Pharm. Res.* 12, 72–81. doi: 10.22159/ijcpr.2020v12i5.39771

Bosmans, F., Aneiros, A., and Tytgat, J. (2002). The sea anemone *Bunodosoma granulifera* contains surprisingly efficacious and potent insect-selective toxins. *FEBS Lett.* 532, 131–134. doi: 10.1016/s0014-5793(02)03653-0

Cardoso, F. C., and Lewis, R. J. (2018). Sodium channels and pain: from toxins to therapies. *Br. J. Pharmacol.* 175, 2138–2157. doi: 10.1111/bph.13962

Casewell, N. R., Wuster, W., Vonk, F. J., Harrison, R. A., and Fry, B. G. (2013). Complex cocktails: the evolutionary novelty of venoms. *Trends Ecol. Evol.* 28, 219–229. doi: 10.1016/j.tree.2012.10.020

Celedon, G., Gonzalez, G., Gulppi, F., Pazos, F., Lanio, M. E., Alvarez, C., et al. (2013). Effect of human serum albumin upon the permeabilizing activity of sticholysin II, a pore forming toxin from *Stichodactyla heliantus*. *Protein J.* 32, 593–600. doi: 10.1007/s10930-013-9521-2

Coulter-Parkhill, A., Dobbin, S., Tanday, N., Gault, V. A., McClean, S., and Irwin, N. (2023). A novel peptide isolated from *Aphonopelma chalcodes* tarantula venom with benefits on pancreatic islet function and appetite control. *Biochem. Pharmacol.* 212, 115544. doi: 10.1016/j.bcp.2023.115544

Coulter-Parkhill, A., McClean, S., Gault, V. A., and Irwin, N. (2021). Therapeutic potential of peptides derived from animal venoms: current views and emerging drugs for diabetes. *Clin. Med. Insights Endocrinol. Diabetes* 14, 11795514211006071. doi: 10.1177/11795514211006071

Da Silva, D. L., Valladao, R., Beraldo-Neto, E., Coelho, G. R., Neto, O., Vigerelli, H., et al. (2023). Spatial distribution and biochemical characterization of serine peptidase inhibitors in the venom of the Brazilian sea anemone *anthopleura cascaia* using mass spectrometry imaging. *Mar. Drugs* 21, 481. doi: 10.3390/md21090481

Deval, E., Noël, J., Lay, N., Alloui, A., Diochot, S., Friend, V., et al. (2008). ASIC3, a sensor of acidic and primary inflammatory pain. *EMBO J.* 27, 3047–3055. doi: 10.1038/emboj.2008.213

Dong, N., Gu, W. W., Yang, L., Lian, W. B., Jiang, J., Zhu, H. J., et al. (2024). MiR-3074-5p suppresses non-small cell lung cancer progression by targeting the YWHAZ/ Hsp27 axis. *Int. Immunopharmacol.* 138, 112547. doi: 10.1016/j.intimp.2024.112547

Erlanger, B. F., Kokorsky, N., and Cohen, W. (1961). The preparation and properties of two new chromogenic substrates of trypsin. *Arch. Biochem. Biophys.* 95, 271–278. doi: 10.1016/0003-9861(61)90145-x

Erturk, G., Hedstrom, M., and Mattiasson, B. (2016). A sensitive and real-time assay of trypsin by using molecular imprinting-based capacitive biosensor. *Biosens. Bioelect.* 86, 557–565. doi: 10.1016/j.bios.2016.07.046

Fautin, D. G. (2009). Structural diversity, systematics, and evolution of cnidae. *Toxicon* 54, 1054–1064. doi: 10.1016/j.toxicon.2009.02.024

Frazao, B., Vasconcelos, V., and Antunes, A. (2012). Sea anemone (Cnidaria, Anthozoa, Actiniaria) toxins: an overview. *Mar. Drugs* 10, 1812–1851. doi: 10.3390/ md10081812

Frias, J., Toubarro, D., Bjerga, G. E. K., Puntervoll, P., Vicente, J. B., Reis, R. L., et al. (2022). A shK-like domain from *steinernema carpocapsae* with bioinsecticidal potential. *Toxins* 14, 754. doi: 10.3390/toxins14110754

Fu, J., Liao, Y., Jin, A. H., and Gao, B. (2021). Discovery of novel peptide neurotoxins from sea anemone species. *Front. Biosci. (Landmark Ed)* 26, 1256–1273. doi: 10.52586/ 5022

Gladkikh, I. N., Klimovich, A. A., Kalina, R. S., Kozhevnikova, Y. V., Khasanov, T. A., Osmakov, D. I., et al. (2023). Anxiolytic, analgesic and anti-inflammatory effects of peptides 1b-2 and hmg 1b-4 from the sea anemone *Heteractis magnifica*. *Toxins (Basel)* 15, 341. doi: 10.3390/toxins15050341

Gomes, P. B., Targino, A. G., Brandão, R. A., and Pérez, C. D. (2016). *Diversity and distribution of actiniaria*. (Springer International Publishing). 125–138. doi: 10.1007/ 978-3-319-31305-4_9

Guo, Q., Fu, J., Yuan, L., Liao, Y., Li, M., Li, X., et al. (2024). Diversity analysis of sea anemone peptide toxins in different tissues of *Heteractis crispa* based on transcriptomics. *Sci. Rep.* 14, 7684. doi: 10.1038/s41598-024-58402-2

Guo, Q.-L., Dai, X.-L., Yin, M.-Y., Cheng, H.-W., Qian, H.-S., Wang, H., et al. (2022). Nanosensitizers for sonodynamic therapy for glioblastoma multiforme: current progress and future perspectives. *Military Med. Res.* 9, 26. doi: 10.1186/s40779-022-00386-z

Hoepner, C. M., Abbott, C. A., and Burke da Silva, K. (2019). The ecological importance of toxicity: sea anemones maintain toxic defence when bleached. *Toxins* 11, 266. doi: 10.3390/toxins11050266

Hoepner, C. M., Stewart, Z. K., Qiao, R., Fobert, E. K., Prentis, P. J., Colella, A., et al. (2024). Proteotransciptomics of the Most Popular Host Sea Anemone *Entacmaea quadricolor* Reveals Not All Toxin Genes Expressed by Tentacles Are Recruited into Its Venom Arsenal. *Toxins (Basel)* 16, 85. doi: 10.3390/toxins16020085

Howe, K., Clark, M. D., Torroja, C. F., Torrance, J., Berthelot, C., Muffato, M., et al. (2013). The zebrafish reference genome sequence and its relationship to the human genome. *Nature* 496, 498–503. doi: 10.1038/nature12111

Hu, B., Guo, W., Wang, L.-h., Wang, J.-g., Liu, X.-y., and Jiao, B.-h. (2011). Purification and characterization of gigantoxin-4, a new actinoporin from the sea anemone *Stichodactyla gigantea*. *Int. J. Biol. Sci.* 7, 729–739. doi: 10.7150/ijbs.7.729

Huang, J., Shi, R., Chen, F., Tan, H. Y., Zheng, J., Wang, N., et al. (2024). Exploring the anti-hepatocellular carcinoma effects of Xianglian Pill: Integrating network pharmacology and RNA sequencing via in silico and *in vitro* studies. *Phytomedicine* 133, 155905. doi: 10.1016/j.phymed.2024.155905

Isaeva, M. P., Chausova, V. E., Zelepuga, E. A., Guzev, K. V., Tabakmakher, V. M., Monastyrnaya, M. M., et al. (2012). A new multigene superfamily of Kunitz-type protease inhibitors from sea anemone *Heteractis crispa*. *Peptides* 34, 88–97. doi: 10.1016/j.peptides.2011.09.022

Jin, X., Wang, Y., Chen, J., Niu, M., Yang, Y., Zhang, Q., et al. (2024). Novel dual-targeting inhibitors of NSD2 and HDAC2 for the treatment of liver cancer: structure-based virtual screening, molecular dynamics simulation, and *in vitro* and *in vivo* biological activity evaluations. *J. Enzyme Inhib. Med. Chem.* 39, 2289355. doi: 10.1080/ 14756366.2023.2289355

John, S. T. (2022). Insecticidal and artemia toxicity of sea anemones *Stichodactyla hadonii* and *anthopleura elegantissima* collected in Kanyakumari coastal waters, gulf of mannar. *Int. J. Innovation Sci. Res. Rev.* 4, 3148–3152.

Kalina, R. S., Peigneur, S., Zelepuga, E. A., Dmitrenok, P. S., Kvetkina, A. N., Kim, N. Y., et al. (2020). New Insights into the Type II Toxins from the Sea Anemone *Heteractis crispa*. *Toxins* 12, 44. doi: 10.3390/toxins12010044

Kanagarajan, U., Bragadeeswaran, S., and Venkatesvaran, K. (2008). On some toxinological aspects of the starfish *stellaster equestris* (Retzius 1805). *J. Venom. Anim. Toxins incl. Trop. Dis.* 14, 435–499. doi: 10.1590/S1678-91992008000300005

Kasheverov, I. E., Logashina, Y. A., Kornilov, F. D., Lushpa, V. A., Maleeva, E. E., Korolkova, Y. V., et al. (2022). Peptides from the sea anemone *metridium senile* with modified inhibitor cystine knot (ICK) fold inhibit nicotinic acetylcholine receptors. *Toxins (Basel)* 15, 28. doi: 10.3390/toxins15010028

Khoo, K. S., Kam, W. K., Khoo, H. E., Gopalakrishnakone, P., and Chung, M. C. (1993). Purification and partial characterization of two cytolysins from a tropical sea anemone, *Heteractis magnifica*. *Toxicon* 31, 1567–1579. doi: 10.1016/0041-0101(93) 90341-f

Kirla, K. T., Erhart, C., Groh, K. J., Stadnicka-Michalak, J., Eggen, R. I. L., Schirmer, K., et al. (2021). Zebrafish early life stages as alternative model to study 'designer drugs': Concordance with mammals in response to opioids. *Toxicol. Appl. Pharmacol.* 419, 115483. doi: 10.1016/j.taap.2021.115483

Koh, C. Y., Modahl, C. M., Kulkarni, N., and Kini, R. M. (2018). Toxins are an excellent source of therapeutic agents against cardiovascular diseases. *Semin. Thromb. Hemost.* 44, 691–706. doi: 10.1055/s-0038-1661384

Kvetkina, A., Malyarenko, O., Pavlenko, A., Dyshlovoy, S., von Amsberg, G., Ermakova, S., et al. (2020). Sea anemone *Heteractis crispa* actinoporin demonstrates *in vitro* anticancer activities and prevents HT-29 colorectal cancer cell migration. *Molecules* 25, 5979. doi: 10.3390/molecules25245979

Kvetkina, A., Pislyagin, E., Menchinskaya, E., Yurchenko, E., Kalina, R., Kozlovskiy, S., et al. (2022). Kunitz-Type Peptides from Sea Anemones Protect Neuronal Cells against Parkinson's Disease Inductors via Inhibition of ROS Production and ATP-Induced P2X7 Receptor Activation. *Int. J. Mol. Sci.* 23, 5115. doi: 10.3390/ijms23095115

Laemmli, U. K. (1970). Cleavage of structural proteins during the assembly of the head of bacteriophage T4. *Nature* 227, 680–685. doi: 10.1038/227680a0

Leychenko, E., Isaeva, M., Tkacheva, E., Zelepuga, E., Kvetkina, A., Guzev, K., et al. (2018). Multigene family of pore-forming toxins from sea anemone *Heteractis crispa*. *Mar. Drugs* 16, 183. doi: 10.3390/md16060183

Li, M., Mao, K., Huang, M., Liao, Y., Fu, J., Pan, K., et al. (2024). Venomics reveals the venom complexity of sea anemone *Heteractis magnifica*. *Mar. Drugs* 22, 71. doi: 10.3390/md22020071

Liao, Q., Feng, Y., Yang, B., and Lee, S. M. (2019a). Cnidarian peptide neurotoxins: a new source of various ion channel modulators or blockers against central nervous systems disease. *Drug Discovery Today* 24, 189–197. doi: 10.1016/j.drudis.2018.08.011

Liao, Q., Gong, G., Poon, T. C. W., Ang, I. L., Lei, K. M. K., Siu, S. W. I., et al. (2019b). Combined transcriptomic and proteomic analysis reveals a diversity of venom-related and toxin-like peptides expressed in the mat anemone Zoanthus natalensis (Cnidaria, Hexacorallia). *Arch. Toxicol.* 93, 1745–1767. doi: 10.1007/s00204-019-02456-z

Logashina, Y. A., Mosharova, I. V., Korolkova, Y. V., Shelukhina, I. V., Dyachenko, I. A., Palikov, V. A., et al. (2017). Peptide from sea anemone *metridium senile* affects transient receptor potential ankyrin-repeat 1 (TRPA1) function and produces analgesic effect. *J. Biol. Chem.* 292, 2992–3004. doi: 10.1074/jbc.M116.757369

Logashina, Y. A., Palikova, Y. A., Palikov, V. A., Kazakov, V. A., Smolskaya, S. V., Dyachenko, I. A., et al. (2021). Anti-inflammatory and analgesic effects of TRPV1 polypeptide modulator APHC3 in models of osteo- and rheumatoid arthritis. *Mar. Drugs* 19, 39. doi: 10.3390/md19010039

Lv, L., Song, K., Xiao, Y., Zheng, J., Zhang, W., Li, L., et al. (2024). Design, synthesis and anticancer activity of beta-carboline based pseudo-natural products by inhibiting AKT/mTOR signaling pathway. *Bioorg. Chem.* 151, 107648. doi: 10.1016/ j.bioorg.2024.107648

Macczak, A., Bukowska, B., and Michalowicz, J. (2015). Comparative study of the effect of BPA and its selected analogues on hemoglobin oxidation, morphological alterations and hemolytic changes in human erythrocytes. *Comp. Biochem. Physiol. C Toxicol. Pharmacol.* 176-177, 62–70. doi: 10.1016/j.cbpc.2015.07.008

Madio, B., King, G. F., and Undheim, E. A. B. (2019). Sea anemone toxins: A structural overview. *Mar. Drugs* 17, 325. doi: 10.3390/md17060325

Madio, B., Peigneur, S., Chin, Y. K. Y., Hamilton, B. R., Henriques, S. T., Smith, J. J., et al. (2018). PHAB toxins: a unique family of predatory sea anemone toxins evolving via intra-gene concerted evolution defines a new peptide fold. *Cell Mol. Life Sci.* 75, 4511–4524. doi: 10.1007/s00018-018-2897-6

Madio, B., Undheim, E. A. B., and King, G. F. (2017). Revisiting venom of the sea anemone *Stichodactyla haddoni*: Omics techniques reveal the complete toxin arsenal of a well-studied sea anemone genus. *J. Proteomics* 166, 83–92. doi: 10.1016/ j.jprot.2017.07.007

Maleeva, E. E., Palikova, Y. A., Palikov, V. A., Kazakov, V. A., Simonova, M. A., Logashina, Y. A., et al. (2023). Potentiating TRPA1 by sea anemone peptide ms 9a-1 reduces pain and inflammation in a model of osteoarthritis. *Mar. Drugs* 21, 167. doi: 10.3390/md21120617

Marks, N., Grynbaum, A., and Lajtha, A. (1973). Pentapeptide (pepstatin) inhibition of brain acid proteinase. *Science* 181, 949–951. doi: 10.1126/science.181.4103.949

Mazzi Esquinca, M. E., Correa, C. N., Marques de Barros, G., Montenegro, H., and Mantovani de Castro, L. (2023). Multiomic approach for bioprospection: investigation of toxins and peptides of Brazilian sea anemone *bunodosoma caissarum*. *Mar. Drugs* 21, 197. doi: 10.3390/md21030197

Melendez-Perez, A. M., Escobar Nino, A., Carrasco-Reinado, R., Martin Diaz, L., and Fernandez-Acero, F. J. (2023). Proteomic Approach to Anemonia sulcata and Its Symbiont *Symbiodinium* spp. as New Source of Potential Biotechnological Applications and Climate Change Biomarkers. *Int. J. Mol. Sci.* 24, 12798. doi: 10.3390/ ijms241612798

Menezes, C., and Thakur, N. L. (2022). Sea anemone venom: Ecological interactions and bioactive potential. *Toxicon* 208, 31–46. doi: 10.1016/j.toxicon.2022.01.004

Mitchell, M. L., Hossain, M. A., Lin, F., Pinheiro-Junior, E. L., Peigneur, S., Wai, D. C. C., et al. (2021). Identification, synthesis, conformation and activity of an insulin-like peptide from a sea anemone. *Biomolecules* 11, 1785. doi: 10.3390/biom11121785

Moghadasia, Z., Shahbazzadeha, D., Jamilib, S., Mosaffa, N., and Bagheria, K. P. (2020). Significant anticancer activity of a venom fraction derived from the Persian gulf sea anemone, *stichodactyla haddoni*. *Iranian J. Pharm. Res.* 19, 402–420. doi: 10.22037/ijpr.2019.14600.12521

Monastyrnaya, M. M., Kalina, R. S., and Kozlovskaya, E. P. (2022). The Sea Anemone Neurotoxins Modulating Sodium Channels: An Insight at Structure and Functional Activity after Four Decades of Investigation. *Toxins (Basel)* 15, 8. doi: 10.3390/toxins15010008

Monastyrnaya, M., Leychenko, E., Isaeva, M., Likhatskaya, G., Zelepuga, E., Kostina, E., et al. (2010). Actinoporins from the sea anemones, tropical *Radianthus macrodactylus* and northern *Oulactis orientalis*: Comparative analysis of structure–function relationships. *Toxicon* 56, 1299–1314. doi: 10.1016/j.toxicon.2010.07.011

Monastyrnaya, M., Peigneur, S., Zelepuga, E., Sintsova, O., Gladkikh, I., Leychenko, E., et al. (2016). Kunitz-type peptide HCRG21 from the sea anemone *Heteractis crispa* is a full antagonist of the TRPV1 receptor. *Mar. Drugs* 14, 229. doi: 10.3390/md14120229

Montaser, R., and Luesch, H. (2011). Marine natural products: a new wave of drugs? *Future Med. Chem.* 3, 1475–1489. doi: 10.4155/fmc.11.118

Moovendhan, M. (2024). Natural pain killers from marine sources: a new frontier in neurosurgical pain management. *Neurosurg. Rev.* 47, 498. doi: 10.1007/s10143-024-02691-8

Moran, Y., Genikhovich, G., Gordon, D., Wienkoop, S., Zenkert, C., Ozbek, S., et al. (2012). Neurotoxin localization to ectodermal gland cells uncovers an alternative mechanism of venom delivery in sea anemones. *Proc. Biol. Sci.* 279, 1351–1358. doi: 10.1098/rspb.2011.1731

Morante, K., Bellomio, A., Viguera, A. R., González-Mañas, J. M., Tsumoto, K., and Caaveiro, J. M. M. (2019). The Isolation of New Pore-Forming Toxins from the Sea Anemone *Actinia fragacea* Provides Insights into the Mechanisms of Actinoporin Evolution. *Toxins* 11, 401. doi: 10.3390/toxins11070401

Park, J. S., Samanta, P., Lee, S., Lee, J., Cho, J. W., Chun, H. S., et al. (2021). Developmental and neurotoxicity of acrylamide to zebrafish. *Int. J. Mol. Sci.* 22, 3518. doi: 10.3390/ijms22073518

Pinheiro-Junior, E. L., Kalina, R., Gladkikh, I., Leychenko, E., Tytgat, J., and Peigneur, S. (2022). A tale of toxin promiscuity: the versatile pharmacological effects of hcr 1b-2 sea anemone peptide on voltage-gated ion channels. *Mar. Drugs* 20, 147. doi: 10.3390/md20020147

Prentis, P. J., Pavasovic, A., and Norton, R. S. (2018). Sea anemones: quiet achievers in the field of peptide toxins. *Toxins (Basel)* 10, 36. doi: 10.3390/toxins10010036

Rachamim, T., Morgenstern, D., Aharonovich, D., Brekhman, V., Lotan, T., and Sher, D. (2015). The dynamically evolving nematocyst content of an anthozoan, a scyphozoan, and a hydrozoan. *Mol. Biol. Evol.* 32, 740–753. doi: 10.1093/molbev/msu335

Raghunathan, C., Raghuraman, R., Choudhury, S., and Venkataraman, K. (2014). Diversity and distribution of sea anemones in India with special reference to Andaman and Nicobar islands. Zoological Survey of India. *Records Zoological Survey India*. 269–294.

Ramezanpour, M., Burke da Silva, K., and Sanderson, B. J. (2012). Differential susceptibilities of human lung, breast and skin cancer cell lines to killing by five sea anemone venoms. *J. Venom. Anim. Toxins including Trop. Dis.* 18, 157–163. doi: 10.1590/S1678-91992012000200005

Ramírez-Carreto, S., Pérez-García, E. I., Salazar-García, S. I., Bernáldez-Sarabia, J., Licea-Navarro, A., Rudiño-Piñera, E., et al. (2019a). Identification of a pore-forming protein from sea anemone *Anthopleura dowii* Verrill, (1869) venom by mass spectrometry. *J. Venom. Anim. Toxins including Trop. Dis.* 25, e147418. doi: 10.1590/1678-9199-jvatitd-1474-18

Ramirez-Carreto, S., Vera-Estrella, R., Portillo-Bobadilla, T., Licea-Navarro, A., Bernaldez-Sarabia, J., Rudino-Pinera, E., et al. (2019b). Transcriptomic and proteomic analysis of the tentacles and mucus of *anthopleura dowii* Verrill 1869. *Mar. Drugs* 17, 436. doi: 10.3390/md17080436

Ravindran, V. S., Kannan, L., and Venkateshvaran, K. (2010). Biological activity of sea anemone proteins: II. Cytolysis and cell line toxicity. *Indian J. Exp. Biol.* 48, 1233–1236.

Ren, H., Chang, L., Su, J., and Jia, X.-z. (2014). Treating Malignant glioma in Chinese patients: update on temozolomide. *OncoTargets Ther* 7, 235–244. doi: 10.2147/ott.S41336

Ren, M., Niu, J., Hu, B., Wei, Q., Zheng, C., Tian, X., et al. (2018). Block of Kir channels by flonicamid disrupts salivary and renal excretion of insect pests. *Insect Biochem. Mol. Biol.* 99, 17–26. doi: 10.1016/j.ibmb.2018.05.007

Rivera-de-Torre, E., Palacios-Ortega, J., Garb, J. E., Slotte, J. P., Gavilanes, J. G., and Martinez-Del-Pozo, A. (2020). Structural and functional characterization of sticholysin

III: A newly discovered actinoporin within the venom of the sea anemone *Stichodactyla helianthus*. *Arch. Biochem. Biophys.* 689, 108435. doi: 10.1016/j.abb.2020.108435

Sakharayapatna Ranganatha, K., Venugopal, A., Chinthapalli, D. K., Subramanyam, R., and Nadimpalli, S. K. (2021). Purification, biochemical and biophysical characterization of an acidic alpha-galactosidase from the seeds of *Annona squamosa* (custard apple). *Int. J. Biol. Macromol.* 175, 558–571. doi: 10.1016/j.ijbiomac.2021.01.179

Salvage, S. C., Rahman, T., Eagles, D. A., Rees, J. S., King, G. F., Huang, C. L., et al. (2023). The beta3-subunit modulates the effect of venom peptides ProTx-II and OD1 on Na(V) 1.7 gating. *J. Cell Physiol.* 238, 1354–1367. doi: 10.1002/jcp.31018

Smith, E. G., Surm, J. M., Macrander, J., Simhi, A., Amir, G., Sachkova, M. Y., et al. (2023). Micro and macroevolution of sea anemone venom phenotype. *Nat. Commun.* 14, 249. doi: 10.1038/s41467-023-35794-9

Subramanian, B., Sangappellai, T., Rajak, R. C., and Diraviam, B. (2011). Pharmacological and biomedical properties of sea anemones *Paracondactylis indicus*, *Paracondactylis sinensis*, *Heteractis magnifica* and *Stichodactyla haddoni* from East coast of India. *Asian Pac J. Trop. Med.* 4, 722–726. doi: 10.1016/S1995-7645(11)60181-8

Suput, D., Frangez, R., and Bunc, M. (2001). Cardiovascular effects of equinatoxin III from the sea anemone *Actinia equina* (L.). *Toxicon* 39, 1421–1427. doi: 10.1016/s0041-0101(01)00102-7

Surm, J. M., Birch, S., Macrander, J., Jaimes-Becerra, A., Fridrich, A., Aharoni, R., et al. (2024). Venom trade-off shapes interspecific interactions, physiology, and reproduction. *Sci. Adv.* 10, eadk3870. doi: 10.1126/sciadv.adk3870

Tajti, G., Wai, D. C. C., Panyi, G., and Norton, R. S. (2020). The voltage-gated potassium channel K(V)1.3 as a therapeutic target for venom-derived peptides. *Biochem. Pharmacol.* 181, 114146. doi: 10.1016/j.bcp.2020.114146

Tonin, G., and Klen, J. (2023). Eptifibatide, an older therapeutic peptide with new indications: from clinical pharmacology to everyday clinical practice. *Int. J. Mol. Sci.* 24, 5446. doi: 10.3390/ijms24065446

Vaghefi, N., Nedjaoum, F., Guillochon, D., Bureau, F., Arhan, P., and Bougle, D. (2002). Influence of the extent of hemoglobin hydrolysis on the digestive absorption of heme iron. An *in vitro* study. *J. Agric. Food Chem.* 50, 4969–4973. doi: 10.1021/jf0109165

Valle, A., Perez-Socas, L. B., Canet, L., Hervis, Y. P., de Armas-Guitart, G., Martins-de-Sa, D., et al. (2018). Self-homodimerization of an actinoporin by disulfide bridging reveals implications for their structure and pore formation. *Sci. Rep.* 8, 6614. doi: 10.1038/s41598-018-24688-2

Vandeputte, M. M., Krotulski, A. J., Walther, D., Glatfelter, G. C., Papsun, D., Walton, S. E., et al. (2022). Pharmacological evaluation and forensic case series of N-pyrrolidino etonitazene (etonitazepyne), a newly emerging 2-benzylbenzimidazole 'nitazene' synthetic opioid. *Arch. Toxicol.* 96, 1845–1863. doi: 10.1007/s00204-022-03276-4

Wang, X., Liao, Q., Chen, H., Gong, G., Siu, S. W. I., Chen, Q., et al. (2021). Toxic peptide from *palythoa caribaeorum* acting on the TRPV1 channel prevents pentylenetetrazol-induced epilepsy in zebrafish larvae. *Front. Pharmacol.* 12. doi: 10.3389/fphar.2021.763089

Windley, M. J., Herzig, V., Dziemborowicz, S. A., Hardy, M. C., King, G. F., and Nicholson, G. M. (2012). Spider-venom peptides as bioinsecticides. *Toxins (Basel)* 4, 191–227. doi: 10.3390/toxins4030191

Yan, F., Cheng, X., Ding, X., Yao, T., Chen, H., Li, W., et al. (2013). Improved Insecticidal Toxicity by Fusing Cry1Ac of *Bacillus thuringiensis* with Av3 of *Anemonia viridis*. *Curr. Microbiol.* 68, 604–609. doi: 10.1007/s00284-013-0516-1

Zaig, S., da Silveira Scarpellini, C., and Montandon, G. (2021). Respiratory depression and analgesia by opioid drugs in freely behaving larval zebrafish. *Elife* 10, e63407. doi: 10.7554/eLife.63407

Zhang, H., Lin, J. J., Xie, Y. K., Song, X. Z., Sun, J. Y., Zhang, B. L., et al. (2023). Structure-guided peptide engineering of a positive allosteric modulator targeting the outer pore of TRPV1 for long-lasting analgesia. *Nat. Commun.* 14, 4. doi: 10.1038/s41467-022-34817-1

Zhang, Y., Zhao, H., Yu, G.-Y., Liu, X.-D., Shen, J.-H., Lee, W.-H., et al. (2010). Structure–function relationship of king cobra cathelicidin. *Peptides* 31, 1488–1493. doi: 10.1016/j.peptides.2010.05.005

Zhao, R., Qasim, A., Sophanpanichkul, P., Dai, H., Nayak, M., Sher, I., et al. (2024). Selective block of human Kv1.1 channels and an epilepsy-associated gain-of-function mutation by AETX-K peptide. *FASEB J.* 38, e23381. doi: 10.1096/fj.202302061R

Zheng, S. X., Chen, J. P., Liang, R. S., Zhuang, B. B., Wang, C. H., Zhang, G. L., et al. (2024). *Schizophyllum commune* fruiting body polysaccharides inhibit glioma by mediating ARHI regulation of PI3K/AKT signalling pathway. *Int. J. Biol. Macromol.* 279, 135326. doi: 10.1016/j.ijbiomac.2024.135326